Rising Temperatures, Rising Risks: A Three-Decade Analysis of Children's Heat Exposure in China (1990-2020)

Kai Feng, Marco M. Laghi, Jere R. Behrman, Emily Hannum, and Fan Wang*

February 1, 2024

Please click here for latest version of the paper.

Abstract

Children are more physically and physiologically vulnerable than adults to the ill effects of climatic and environmental shocks such as heat waves. There is a growing evidence linking extreme heat exposure to poorer developmental outcomes for children in domains ranging from education to health to long-term productivity. The frequency and intensity of heat waves are increasing as the earth's climate warms, but how these trends translate to changes in children's heat exposure is not well established. Changes in children's heat exposure are a joint function of changes in temperature and its geographic distribution and changes in the geographic distribution of the child population. Most studies that estimate the population burden of extreme heat 1) have focused on the total burden measured as person-time while overlooking within-population heterogeneities; 2) have not specifically focused on child populations; 3) have not explicitly attended to changing population distributions over time; 4) have relied on average temperature approaches without considering large hourly, daily and monthly temperature variations; and 5) have not estimated exposures at different, health-relevant temperature thresholds.

Using the case of China, the world's most populous country over the three recent decades studied, this paper estimates children's changing exposure to extreme high temperatures by linking county-level child population data to hourly Universal Thermal Climate Index (UTCI) data across two censuses spanning 30 years (1990-2020). We propose a convenient, low-data-demand framework for estimating the share of children at risk of extreme temperature exposures that 1) jointly considers temperature thresholds and the share of time exposed to such temperature thresholds, 2) jointly considers the geographical and temporal distributions of temperature and of children, and 3) allows for estimates for more and less extreme thresholds. Applying this framework to China, we find substantial increases in the average high-heat exposure for children and the share of children at risk and substantial regional heterogeneities. We also find that approximately half of the overall change in child high-heat exposure between 1990 and 2020 is driven by heat increases and the rest is driven by shifts in child population towards locations that have higher temperatures, illustrating the importance of paying attention to population distribution in addiion to temperature patterns.

Keywords: Extreme temperature, children

*Kai Feng: Department of Sociology and Population Studies Center, University of Pennsylvania, Philadelphia, Pennsylvania, USA; Marco M. Laghi: Department of Sociology, New York University, New York, NY, USA; Center for Applied Social and Economic Research, NYU Shanghai, Shanghai, China; Jere R. Behrman: Departments of Economics and Sociology and Population Studies Center, University of Pennsylvania, Philadelphia, Pennsylvania, USA; Emily Hannum: Department of Sociology and Population Studies Center, University of Pennsylvania, Philadelphia, Pennsylvania, USA; Fan Wang: Department of Economics, University of Houston, Houston, Texas, USA. This paper is supported by National Science Foundation Grants 1756738 and 2230615.

1 Introduction

Nearly half of the world's children live in countries identified by UNICEF's Children's Climate Risk Index as high-risk (UNICEF 2021), and children are highly physically and physiologically susceptible to climate-related disasters, hazards,[1] and diseases. For example, children are highly vulnerable to daily thermo-regulatory stress and other health problems when exposed to extreme temperatures (Smith 2019; UNICEF 2021; Xu et al. 2012), and their education can also be affected (Park, Behrer, and Goodman 2020). Growing evidence suggests that heat exposure affects children's short- and long-term development and welfare outcomes, from education to health to long-term productivity. This body of work includes emerging literature in China, which is home to more than 253.38 million children ages 0-14 in the year 2020 (National Bureau of Statistics of China 2021). In China, extreme-heat exposure has been linked to health outcomes including lower birthweights, more preterm birth, the common cold, hand, foot, and mouth diseases, and asthma (Guo et al. 2012; Liu et al. 2022; Lu et al. 2022; Lu et al. 2018; Ren et al. 2023; Xu et al. 2015), and extreme temperatures have also been linked to poorer academic performance (Jiang et al. 2018; Wang et al. 2018). And while the intersection of temperature and bodily development is less studied, Lai et al. (2023) and Zivin and Shrader (2016) review cross-country evidence suggesting that extreme temperatures experienced at an early age can limit bodily development and thus work productivity as an adult.

In short, research from China and elsewhere suggests that rising temperatures and associated increases in heat spells could have negative implications for children across a range of important life domains. However, studies have not yet not rigorously established the extent to which heat exposure among children has been changing. To do so requires attention not only to identifying where and how much temperatures have changed, but also to where children live and, importantly, to the possibility of changes over time in the geographical distribution of the child population. A line of research on China, unlinked to population data, has shown an increase in the frequency of yearly high heat exposure days, with the highest intensities occurring outside of the North (Li and Zha 2020). A separate body of work has considered the average population burden of heat exposure (Chen, He, and Zhang 2023; Zhan et al. 2018; Zhang et al. 2020), with some studies decomposing sources of increased heat exposure (Jones et al. 2018), and some considering region-specific patterns and trends (Li and Zha 2020; Shi et

1. For reviews of heat exposure effects and effects of other climatic hazards on children, see Connon and Dominelli (2022a, 2022b)

al. 2021; Sun et al. 2020). However, little work has focused specifically on estimating exposure levels and changes in the child population and none has considered the potential interactions between shifts in the distribution of child population and distributions of heat exposure across locations over time. With unprecedented internal migration in China in recent decades, the contributions of shifting geographical distribution of children to their heat exposure could be substantial.

This paper links county-specific child population counts from Chinese censuses to hourly temperature data to estimate ambient heat-exposure risk for children between 1990 and 2020, incorporating geographic and temporal distributions of heat and the population of children. We propose a framework for measuring the share of children at risk of extreme temperature exposures that jointly considers 1) various temperature thresholds and 2) the share of time exposed to extreme heat using those temperature thresholds. In addition to attending to changes in the geographic distribution of the child population over time, this framework improves on many prior estimates of population burdens of heat exposure by 1) capitalizing on temporally dis-aggregated data that allows consideration of significant heterogeneities in hourly variations in temperatures across space and 2) allowing for estimation of exposure burdens at different temperature thresholds thought to be relevant to human health and functioning.[2]

Results from this exercise show substantial increases in average heat exposure for children and the share of children at risk. Half of the overall change in child heat exposure between 1990 and 2020 is attributable to heat increases. There is substantial regional heterogeneity, with much of the national increase in child exposure to extreme heat attributable to changes in the Eastern region. Most importantly, this analysis reveals that about half of the rising exposure to heat among children is driven by shifts in the child population toward locations that have higher temperatures.

2. A number of mortality studies in China have used temperature data. Zeng et al. (2022) considers age-specific disparities in temperature-driven mortality, using the 2000 and 2010 censuses. Zeng et al. finds youth to lose more years of life from increased heat compared to elders, although they do acknowledge a lack of analysis of child ages specifically in their study. Liao et al. (2023) goes further in observing mortality, utilizing census data from 2000-2010 and breaking up the analysis into China's counties. They find that increased daily maximum temperature increases monthly mortality rate across counties by about 1.7%. However, Liao et al. (2023) does not focus on children as uniquely vulnerable population.

2 Background

In studies that consider population heat exposures, a prevalent metric for assessing heat exposure is the change in exposure in total person-time. Person-time exposure statistics are determined by both the population count and the duration of exposure to a specific risk factor over a given period in a particular location.[3] An aggregate statistic for a region or country is computed by summing person-time across locations within the region or country. While aggregate person-time serves as a valuable estimate for measuring the overall burden on a population, it has two limitations. First, when comparing exposures over time, aggregate person-time statistics will capture changes in aggregate population size over time in addition to changes in average heat exposure burdens. This situation makes results harder to interpret. For example, if the rate of population decline surpasses the rate of temperature increase, the resultant person-time estimates may diminish over time. Second, the person-time aggregate provides a single statistic of exposure for a region or country, overlooking the heterogeneities in ambient exposure changes across populations residing in locations with differing climatic change experiences. We propose a distributional approach to estimate the heterogeneities in changes of the percentages of children's time under heat stress.

Zhang et al. (2020) runs multiple projections to examine long-term extreme-heat temperature exposure but only during China's warm season weighed by general population growth, using fine-resolution data and finding a projected increase in heat exposure in comparison to projected spatially-weighted temperature data. A paper by Spangler, Liang, and Wellenius (2022) presents a relevant meteorological data set in the United States context using hourly temperature extremes and the Universal Thermal Climate Index (UTCI) calculated and weighed at the county-population level for the 21st century. However, many studies suffer from a high level of geographic or temporal aggregation of their data. For example, the United Nations Children's Fund (2022) focuses on increasing durations of global heatwaves and projections for the future, using daily maximum temperatures to visualize global exposures for children using admittedly low-resolution data. These studies demonstrate the underutilized potential of current climate data analysis that our framework seeks to rectify by digging deeper into population-specific and person-time statistics.

3. The person-days of heat exposure in a place at time t can be computed, for example, by multiplying the days where the maximum temperature exceeds a threshold level with the total population residing in a place at time t.

3 Methods and Data

Methods. In this section, we summarize our framework and method for measuring child population at risk of heat exposure. Within a particular span of time in a region, our framework develops two statistics of temperature exposure risks building on two types of distributions and two types thresholds. The two distributions are the distribution of location-specific temperature and the distribution of population across locations conditional on population group (children). The two thresholds are temperature thresholds for extreme-temperature exposure and time thresholds for share of time exposed to extreme-temperature. The first risk statistics captures the risk of extreme temperature facing the average child, measured in units of share of time the average child is exposed to extreme temperature. The second risk statistics capture the distribution of risk among children, measured in units of the share of child population exposed to extreme temperatures for different durations of time.

In the closest related work, United Nations Children's Fund (2022) estimates the aggregate number of children at risk of heat exposure based on the aggregate-population share of children. The closest related works focusing on all population groups generally provide different types of average aggregated statistics. Our framework is the first to jointly apply the double-distributions to compute the share of children (and population generally) at risk of the double-thresholds of exposure. We provide a detailed description of our methods in the appendix.

We implement our framework in the setting of China between 1990 and 2020. In this empirical application, we consider each span of time as one year, we approximate continuous ambient temperature exposure based on hourly estimates of temperature, and we approximate fine-grained measures of locations where the temperature gradient is non-zero with counties (3rd level administrative units) in China. For the temperature thresholds, we consider a range of thresholds but focus our analysis on key thresholds for extreme-heat commonly used in the literature. For time thresholds, we consider different shares of time during the course of the year exposed to temperatures above the thresholds considered. Our method is also straightforward to implement in other settings where tabular population data at relatively fine-grained level and location-specific climate data is available.

Data. In terms of climate data, we utilize the fifth generation of the European Centre for Medium-Range Weather Forecasts (ECMWF) atmospheric reanalyses of the global climate: the

ERA5-HEAT dataset (Napoli 2020). ERA5-HEAT, a distinct advancement from its predecessors, offers hourly data on numerous climate variables with a spatial resolution of 0.25 degrees one of which we utilize is Universal Thermal Climate Index (UTCI). UTCI provides an integrative measure of the human-perceived equivalent temperature, taking into account factors like air temperature, humidity, wind speed, and radiant heat (Bröde et al. 2012; Jendritzky, Dear, and Havenith 2012; Jendritzky and Höppe 2017).

For population data, we utilize Chinese census data for the years 1990 and 2020 (All China Market Research Ltd 2022; Beijing Hua tong ren shi chang xin xi you xian ze ren gong si 2005a, 2005b; China Data Lab 2020). County-level population data, shapefiles, and microdata on demographic characteristics of age and gender were extracted and used to construct the population exposures by county.

For regional analysis, temperature and population data were sorted by province and assigned a region according to the four recognized economic regions of China (National Bureau of Statistics of China 2011).

4 Results

Aggregate Average Changes in Extreme Temperature Burdens over Time for Cohorts of Children. The complexities of living under a dynamic anthropocentric context have necessitated expanding and reconsidering how people experience extreme heat. Arbuthnott et al. (2016) systematically reviews the literature and finds evidence to believe that exposure susceptibility to high temperatures, in relation to mortality, has lowered for persons depending on location, pointing to an element of dynamic climate adaptation. The Universal Thermal Climate Index (UTCI) is another example of consideration of human-experienced climate change. Developed at the beginning of the 21st century by the International Society of Biometeorology, the UTCI is an index used for comprehensively measuring the interaction of the thermal environment upon the human body (Bröde et al. 2012; Jendritzky, Dear, and Havenith 2012; Jendritzky and Höppe 2017). The benefit of UTCI over other measures is UTCI's sensitivity to fluctuations while still maintaining high correlations to some, but not all other types of temperature indexes (Blazejczyk et al. 2012; Bröde et al. 2018; Spangler et al. 2023). UTCI lends towards a consideration of ambient temperature as it is actually humanly experienced, supporting a greater development in the literature towards recognizing population-weighted

exposures rather than defaulting to spatially-based measurements (Gao et al. 2018; Kyaw et al. 2023; Spangler, Liang, and Wellenius 2022).

When the UTCI is above 26°C, it indicates a moderate or higher level of thermal stress on the human body. As the UTCI value increases, the level of thermal stress on the human body intensifies. Figure 1 depicts an increase in temperature exposure for children ages 0 to 14 across mainland China from 1990 to 2020. Focusing on 26°C, a temperature level that is considered to be associated with moderate or stronger heat stress, an average child in China experienced 20.09% of her total ambient hours in 1990 at equal to or above this threshold. By 2020, this percentage increased to 22.81% (Figure 1), representing a 2.72 percentage points and 13.54 % increase in annual average exposure duration, which corresponds to an annual average increase of 238 hours of additional ambient moderate or stronger heat stress exposure over 30 years.

Additionally, on average in 2020, children experience 8.26% and 1.16% of their annual ambient hours—marking 14.70% and 10.64% increases compared to 1990—at over 32°C and 38°C, which are temperature levels marking thresholds for strong and very strong heat stress. This nationwide increase will be further inspected in the following sections to understand more local implications of UTCI change.

To situate the contribution of our framework and results utilizing exposure of child populations across China to distributions of temperature over time, we first outline other temperature exposure literature. Literature focusing on temperature exposure can be grouped into one of three categories. The first is literature that observes high-temperature trends in a location across time, such as in China, without a specific focus on its population. Luo and Lau (2019) computes temperature readings from weather stations to depict long-term trends of increasing summer heat stress across China's geography without directly taking into consideration administrative boundaries or the populations within them. Luo and Lau (2018) similarly uses station data and zooms in to find increased heat stress spatially concentrated around urban centers. These works are limited to only considering space and not population. At most, this literature mentions that certain areas of a nation are more densely populated than others without actually including population counts in their exposure calculation.

The second literature on heat exposure over time roughly approximates location-based populations using Chinese national and grouped provincial borders to estimate broad population exposure. The limitations of United Nations Children's Fund (2022) have already been noted,

namely that while it uniquely focuses on children its usage of national aggregate data prevents further utility. Freychet et al. (2022) uses country-level population and national growth in projecting future heat risk, finding increasingly high experienced risk as temperatures increase but only calculating this risk based on nation-level population. Zhan et al. (2018) is slightly more detailed, finding differing levels of increased population heat exposure projected overtime on the regional level. While this literature provides some empirical context for heat exposure for a population over time compared to the first set of literature, population variation is liable to differ across even a single province let alone the regions and China as a whole.

A third literature is more exact in attributing heat exposure to localized counts of populations over time. This third category has been the most advanced iteration thus far in the literature. Li and Zha (2020) for example uses county-level population data to find exposure over time to extreme heat days in the summer, finding broad increases in risk with particular hot spots in counties in East, South, and Central China. Chen, He, and Zhang (2023), Kennard et al. (2022), and Ning et al. (2023) all use gridded temperature and population data to find increased experienced days of heat risk driven in part by population distribution over time. However, even in this more advanced literature, a true distribution of time during which extreme heat is experienced is eschewed for daily summary measures.

Literature on heat exposure has gotten more nuanced in its consideration of population except in consideration of special populations, like children. Further, temperature distribution over time has been under-considered until now. All three types of literature suffer from their utilization of summary statistic measures of temperature: mean and maximum temperatures. These measures are naive to how human beings experience temperature throughout time. By utilizing population distribution and temperature distribution over time, we see for the first time with great detail who is actually at risk as a result of increased temperature trends. Next, we will show that our contribution offers a critical foundation for outcome-focused literature as well. Building upon the exposure literature, our research is the first to show in detail an increasing share of time that child populations across China face extreme heat in their immediate surroundings.

Increases in Share of Children at Risk of Heat Exposure. While the previous results focus on heat exposure for the average child in China, it does not provide information on how many children are increasingly at risk of heat exposure. In this section, given the distribution of heat

and children across counties in China, we examine whether the *percentage* of children most affected by heat stress has also changed over time.

As discussed in the methods section, we compute the share of children at risk by considering jointly two thresholds of risks: a threshold for temperature and also a threshold for the share of time (hours) exposed to temperature above a particular threshold. In Figure 2, we consider different levels of temperature as well as shares of time thresholds, providing different measures of changes in the share of children at risk depending on plausible considerations of thresholds for risks.

Here we consider two ends of the risk spectrum. First, we consider a lower temperature threshold combined with a higher share of hours, then a higher temperature threshold combined with a lower share of hours. Then, at the bottom left direction of each sub-figure in Figure 2, in 1990, 9.49% of children experienced moderate or stronger heat stress (i.e. UTCI above 26°C) for over 30% of their hours. By 2020, this number had risen to 19.51%, marking an increase of 10.02 percentage points. In other words, the share of children experiencing heat stress for at least 30% of their total hours in 2020 almost doubled compared to 1990. Second, at the top right direction of each sub-figure in Figure 2, in 1990, 17.45% of children have at least 10% of their total hours that are above 32°C. This number rose to 23.55% in 2020, representing a 6.10 percentage point or 34.96% increase. Overall, by both at-risk standards, approximately one-quarter of children in China are at-risk of extreme heat exposure in 2020, increasing from about only one-sixth of children in 1990.

Additionally, Figure 2 also shows alarmingly fast increases in the share of children at risk toward the direction (lower right of Figure 2) of increasing risk. In particular, the share of children experiencing at least 30 percent of annual ambient time at over 29°C and 20 percent of time at over 31°C increased from 0.02% and 0.25% in 1990 to 1.37% and 1.39% in 2020, respectively. While the share of children exposed at these extreme risk levels remain small, these increases represent approximately 60-fold and 5-fold jumps in the share of children at these high exposure risk levels, respectively.

In observing thresholds of risk being surpassed over time we provide important context on the increasing risk being faced by China's children. Much literature has focused on child health and development outcomes being negatively affected by increases in temperature over time, including: preterm birth (Ren et al. 2023), low birth weight (Liu et al. 2022), and a growing list of other negative health outcomes mentioned throughout this paper's introduction.

This growing outcome literature is important but has lacked until now a foundational basis to observe which children are actually at risk of the outcomes being researched. This research gap is especially problematic due to a lack of exposure-over-time literature focusing on child populations. Here we create the opportunity to ground the child outcome-focused literature and observe the development of experienced risk over time. Our contribution is especially powerful as we provide multiple thresholds of temperature and time to depict levels of risk severity. Our novel framework can easily be adapted to other research contexts and can be extended to other national settings or populations of interest.

Decomposing the Contributions of Changes in Temperature and Population. Figure 3 depicts a counterfactual decomposition analysis against the UTCI experienced by populations in 1990 and 2020. This counterfactual decomposition shows the extent to which change in exposure is due to population change, or due to change in UTCI as a result of meteorological change.

We first present the percentage gap between year 2020 and 1990 (as indicated by the red line). As mentioned above, we observed a 2.7% increase in children's exposure to moderate or stronger heat stress (the vertical line indicates the critical UTCI threshold of 26°C). We then conduct the first counterfactual analysis (green line: climate effect), which combines the children population distribution in 2020 with the observed temperature in 1990. We take the percentage deviation of the counterfactual results from the original results in 1990. In the second counterfactual analysis (blue line: population effect), we use children population distribution in 1990 with the observed temperature in 2020, and again we take the percentage deviation of the results from the original results in 1990. We find that the population effect and climate effect are almost identical after the 26°C UTCI threshold. It implies that the change in child population distribution and temperature equally contribute to an increase in children's exposure to heat stress at this level.

We note a unique contribution we provide via our decomposition in focusing on the historic attribution of temperature exposure and its change in China from 1990 to 2020. Sparse literature exists that performs decomposition analysis in China's past data context. Sun et al. (2008) performs a historic decomposition of weather station temperature data into regions, finding Northern China to be most significantly contributing to overall temperature increases in the country over time. However, this study again only considers space and not population. Dong,

Tao, and Zhang (2023) provides a rich but geographically limited historical case study of heatwaves in the Xinjiang Province from 1961 to 2020. Dong, Tao, and Zhang (2023) decomposes temperature exposure into population effect, climate effect, and the interaction of the two, finding that since 1961 population effects have become increasingly important and climate less so. Emphasizing the flexibility of data utilization in our analyses, including counterfactual and decomposition analyses, we find comparable regional historical results. We also showcase, likely for the first time, China's overall historical climate and child population-decomposed temperature exposure trends from 1990 to 2020.

Changes in Children's Heat Exposure Across Regions. Results pictured in Figure 4 depict the difference in regionally experienced UTCI for children ages 0 to 14 across China in the years 1990 and 2020, using hourly temperature data. Our regional results show changes in heat exposure determined by county change but not region change, as opposed to our national results which do both.

Panel A in Figure 4 displays the cumulative density curve of hourly exposure to a specified UTCI (Universal Thermal Climate Index) threshold, ranging from -40°C to 40°C, across the years 1990 to 2020. This curve represents data for four distinct economic regions. A vertical line is drawn at 26°C, marking the threshold above which conditions are considered to represent moderate or higher levels of heat stress.

Panel B in Figure 4 presents the percentage point deviation between the cumulative density curve in 1990 and 2020 after 26°C by region. It highlights that the national increase in child exposure to extreme heat from 1990 to 2020 shown in Figure 1 is primarily attributed to changes in the Eastern region, with notable but smaller contributions from the Northeastern and Central regions.

For example, an average child in Eastern China was exposed to moderate or more severe heat stress for 23.65% of their total hour in 1990. By 2020, this percentage increased to 28.09%, representing 18.77% increase in annual average exposure or 389 hours of additional heat stress exposure.

We showcase for the first time regional variation for temperature exposure on child populations over time. We provide an extra layer of nuance to other literature that emphasizes regional differences in temperature exposure over time. For example, Ning et al. (2023) and Sun et al. (2020) both find regional nuance in heatwaves, with Southeast China experiencing hotter

heatwaves but Northeast China experiencing more frequent incidences of heatwaves. Shi et al. (2021) observes regional changes in heating and cooling, making their case for degree-hours as a measure by showing temperature progression across years at different times of day. Li and Zha (2020) is especially effective in finding Northern China experiencing the least increase in heat risk days compared to other regions. These and other examples of existing literature (Dong, Tao, and Zhang 2023; Xiao et al. 2017; Yang et al. 2021; Zhao et al. 2018), leave gaps in the form of long-term observation of temperature exposure on populations across individual provinces of China. Our research framework fills in these gaps, offering a more holistic view of temperature distribution and allowing for zooming into national and regional child population contexts, to understand for the first time the regional heat risk children have been facing over time in China.

5 Discussion and Conclusion

In this paper, we combined county-level census population data on child distribution from 1990 and 2020 with temperature data to study changes in ambient heat exposure facing children over three decades. We find substantial increases in the average heat exposure for children and the share of children at risk and substantial regional heterogeneity. Interestingly, we find that half of the overall changes in high child heat exposure are driven by heat increases and the rest is driven by shifts in child population towards locations that have higher temperatures.

In our first result, we found that in 1990, an ***average*** child in China experienced moderate or stronger heat stress (UTCI 26°C and above) for 20.09 % of their hours. By 2020, this percentage had increased by 2.7 percentage points (pp) (Figure 1). In our second result, we found that in 1990, 9.49 % of children experienced moderate or stronger heat stress for over 30 % of their hours. By 2020, this figure had risen to 19.51 %, marking an increase of 10.02 pp (Figure 2).

For our third result, counterfactual decomposition analyses reveal that the effects of escalating temperatures and a growing child population in the heat-affected regions contribute equally to the overall increase in heat exposure among children (Figure 3). For the fourth result, the substantial increase in children's exposure to heat stress in Eastern China, the nation's most economically developed and densely populated region, is a primary driver behind the overall surge observed at the national level (Figure 4).

We implicitly assume uniform sensitivity and adaptability to heat stress among all individuals, overlooking the potential adaptability of those residing in warmer regions. Our definition of heat exposure is simplified, and future research could adopt the same methodology with different definitions of heat stress. For instance, exploring heat wave episodes rather than focusing solely on single hours above the heat stress threshold could provide a more comprehensive understanding. Additionally, while our focus is on total hours, it's important to acknowledge that children may tend to stay indoors with air conditioners during heat waves, and the ability to withstand heat stress may vary by socioeconomic status. Lastly, despite utilizing county-level data, a more granular measure may better capture heat stress even using our same framework, particularly in urban areas where factors like the heat island effect come into play.

References

All China Market Research Ltd. 2022. *2020 China County Population Census Data with GIS Maps.*

Arbuthnott, Katherine, Shakoor Hajat, Clare Heaviside, and Sotiris Vardoulakis. 2016. "Changes in Population Susceptibility to Heat and Cold Over Time: Assessing Adaptation to Climate Change." *Environmental Health* 15 (S1): S33. https://doi.org/10.1186/s12940-016-0102-7.

Beijing Hua tong ren shi chang xin xi you xian ze ren gong si. 2005a. *1990 County Boundaries of China with Population Census Data, Part 1 & 2. [Shapefile].* https://geo.nyu.edu/catalog/nyu-2451-34775.

———. 2005b. *China Historical 2000 County Population Census Data.* https://geo.nyu.edu/catalog/harvard-ch-census2000.

Blazejczyk, Krzysztof, Yoram Epstein, Gerd Jendritzky, Henning Staiger, and Birger Tinz. 2012. "Comparison of UTCI to Selected Thermal Indices." *International Journal of Biometeorology* 56, no. 3 (May): 515–535. https://doi.org/10.1007/s00484-011-0453-2.

Bröde, Peter, Dusan Fiala, Krzysztof Błażejczyk, Ingvar Holmér, Gerd Jendritzky, Bernhard Kampmann, Birger Tinz, et al. 2012. "Deriving the Operational Procedure for the Universal Thermal Climate Index (UTCI)." *International Journal of Biometeorology* 56, no. 3 (May 1, 2012): 481–494. https://doi.org/10.1007/s00484-011-0454-1.

Bröde, Peter, Dusan Fiala, Bruno Lemke, and Tord Kjellstrom. 2018. "Estimated Work Ability in Warm Outdoor Environments Depends on the Chosen Heat Stress Assessment Metric." *International Journal of Biometeorology* 62, no. 3 (March): 331–345. https://doi.org/10.1007/s00484-017-1346-9.

Chen, Huopo, Wenyue He, and Shuhui Zhang. 2023. "Recent Urbanization Increases Exposure to Humid-Heat Extreme Events Over Populated Regions of China." *Atmospheric and Oceanic Science Letters* (August 25, 2023): 100409. https://doi.org/10.1016/j.aosl.2023.100409.

China Data Lab. 2020. *China County Map with 2000-201o Population Census Data.* In collaboration with China Data Lab. https://doi.org/10.7910/DVN/VKGEBX.

Connon, Irena, and Lena Dominelli. 2022a. *Rapid Literature Review: Children and Heat Waves.* UNICEF Children's Climate Change Risk Index (CCRI). Data for Children Collaborative, September. https://www.dataforchildrencollaborative.com/outputs/rapidreview-heatwaves-tmha3.

———. 2022b. *Systematic Review of the Literature: Findings, Outcomes and Policy Recommendations.* UNICEF Children's Climate Change Risk Index (CCRI). Data for Children Collabortive and UNICEF, April. http://dspace.stir.ac.uk/handle/1893/34193.

Dong, Diwen, Hui Tao, and Zengxin Zhang. 2023. "Historic Evolution of Population Exposure to Heatwaves in Xinjiang Uygur Autonomous Region, China." *Scientific Reports* 13, no. 1 (May 6, 2023): 7401. https://doi.org/10.1038/s41598-023-34123-w.

Freychet, Nicolas, Gabriele C. Hegerl, Natalie S. Lord, Y. T. Eunice Lo, Dann Mitchell, and Matthew Collins. 2022. "Robust Increase in Population Exposure to Heat Stress with Increasing Global Warming." *Environmental Research Letters* 17, no. 6 (June): 064049. https://doi.org/10.1088/1748-9326/ac71b9.

Gao, Xue-Jie, Jie Wu, Ying Shi, Jia Wu, Zhen-Yu Han, Dong-Feng Zhang, Yao Tong, et al. 2018. "Future Changes in Thermal Comfort Conditions Over China Based on Multi-regcm4 Simulations." *Atmospheric and Oceanic Science Letters* 11, no. 4 (July 4, 2018): 291–299. https://doi.org/10.1080/16742834.2018.1471578.

Guo, Yuming, Fan Jiang, Li Peng, Jun Zhang, Fuhai Geng, Jianming Xu, Canming Zhen, et al. 2012. "The Association Between Cold Spells and Pediatric Outpatient Visits for Asthma in Shanghai, China." *PLOS ONE* 7, no. 7 (July 25, 2012): e42232. https://doi.org/10.1371/journal.pone.0042232.

Jendritzky, Gerd, Richard de Dear, and George Havenith. 2012. "UTCI—Why Another Thermal Index?" *International Journal of Biometeorology* 56, no. 3 (May 1, 2012): 421–428. https://doi.org/10.1007/s00484-011-0513-7.

Jendritzky, Gerd, and Peter Höppe. 2017. "The UTCI and the ISB." *International Journal of Biometeorology* 61, no. 1 (September 1, 2017): 23–27. https://doi.org/10.1007/s00484-017-1390-5.

Jiang, Jing, Dengjia Wang, Yanfeng Liu, Yanchao Xu, and Jiaping Liu. 2018. "A Study on Pupils' Learning Performance and Thermal Comfort of Primary Schools in China." *Building and Environment* 134 (April 15, 2018): 102–113. https://doi.org/10.1016/j.buildenv.2018.02.036.

Jones, Bryan, Claudia Tebaldi, Brian C. O'Neill, Keith Oleson, and Jing Gao. 2018. "Avoiding Population Exposure to Heat-Related Extremes: Demographic Change Vs Climate Change." *Climatic Change* 146, no. 3 (February 1, 2018): 423–437. https://doi.org/10.1007/s10584-017-2133-7.

Kennard, H., T. Oreszczyn, M. Mistry, and I. Hamilton. 2022. "Population-Weighted Degree-Days: The Global Shift Between Heating and Cooling." *Energy and Buildings* 271 (September 15, 2022): 112315. https://doi.org/10.1016/j.enbuild.2022.112315.

Kyaw, Aung Kyaw, Mohammed Magdy Hamed, Mohammad Kamruzzaman, and Shamsuddin Shahid. 2023. "Spatiotemporal Changes in Population Exposure to Heat Stress in South Asia." *Sustainable Cities and Society* 93 (June 1, 2023): 104544. https://doi.org/10.1016/j.scs.2023.104544.

Lai, Wangyang, Yun Qiu, Qu Tang, Chen Xi, and Peng Zhang. 2023. "The Effects of Temperature on Labor Productivity." *Annual Review of Resource Economics* 15 (1): 213–232. https://doi.org/10.1146/annurev-resource-101222-125630.

Li, Long, and Yong Zha. 2020. "Population Exposure to Extreme Heat in China: Frequency, Intensity, Duration and Temporal Trends." *Sustainable Cities and Society* 60 (September): 102282. https://doi.org/10.1016/j.scs.2020.102282.

Liao, Hua, Chen Zhang, Paul J. Burke, Ru Li, and Yi-Ming Wei. 2023. "Extreme Temperatures, Mortality, and Adaptation: Evidence from the County Level in China." *Health Economics* 32, no. 4 (April): 953–969. https://doi.org/10.1002/hec.4649.

Liu, Xiaoying, Jere Behrman, Emily Hannum, Fan Wang, and Qingguo Zhao. 2022. "Same Environment, Stratified Impacts? Air Pollution, Extreme Temperatures, and Birth Weight in South China." *Social Science Research* 105 (July 1, 2022): 102691. https://doi.org/10.1016/j.ssresearch.2021.102691.

Lu, Chan, Zijing Liu, Hongsen Liao, Wenhui Yang, Qin Liu, Qin Li, and Qihong Deng. 2022. "Interaction of Exposure to Outdoor Air Pollution and Temperature During Pregnancy on Childhood Asthma: Identifying Specific Windows of Susceptibility." *Building and Environment* 225 (November 1, 2022): 109676. https://doi.org/10.1016/j.buildenv.2022.109676.

Lu, Chan, Yufeng Miao, Ji Zeng, Wei Jiang, Yong-Ming Shen, and Qihong Deng. 2018. "Prenatal Exposure to Ambient Temperature Variation Increases the Risk of Common Cold in Children." *Ecotoxicology and Environmental Safety* 154 (June): 221–227. https://doi.org/10.1016/j.ecoenv.2018.02.044.

Luo, Ming, and Ngar-Cheung Lau. 2019. "Characteristics of Summer Heat Stress in China During 1979–2014: Climatology and Long-Term Trends." *Climate Dynamics* 53, no. 9 (November 1, 2019): 5375–5388. https://doi.org/10.1007/s00382-019-04871-5.

Luo, Ming, and Ngar-Cheung Lau. 2018. "Increasing Heat Stress in Urban Areas of Eastern China: Acceleration by Urbanization." *Geophysical Research Letters* 45, no. 23 (December 16, 2018). https://doi.org/10.1029/2018GL080306.

Napoli, Claudia Di. 2020. *Thermal Comfort Indices Derived from ERA5 Reanalysis.* https://doi.org/10.24381/CDS.553B7518.

National Bureau of Statistics of China. 2011. *[Method of Dividing the East, West, Central and Northeast Regions].* Beijing: State Council of China, June 13, 2011. https://web.archive.org/web/20190323041213/http://www.stats.gov.cn/ztjc/zthd/sjtjr/dejtjkfr/tjkp/201106/t20110613_71947.htm.

———. 2021. *Main Data of the Seventh National Population Census.* Beijing: State Council of China, May 11, 2021. https://www.unicef.cn/en/media/24511/file/What%20the%202020%20Census%20Can%20Tell%20Us%20About%20Children%20in%20China%20Facts%20and%20Figures.pdf.

Ning, Xiaoju, Yuanzheng Li, Genghe Gao, Yan Zhang, and Yaochen Qin. 2023. "Temporal and Spatial Characteristics of High Temperatures, Heat Waves, and Population Distribution Risk in China from 1951 to 2019." *Environmental Science and Pollution Research* 30, no. 42 (September 1, 2023): 96629–96646. https://doi.org/10.1007/s11356-023-28955-2.

Park, R. Jisung, A. Patrick Behrer, and Joshua Goodman. 2020. "Learning is Inhibited by Heat Exposure, Both Internationally and Within the United States." *Nature Human Behaviour* 5, no. 1 (October 5, 2020): 19–27. https://doi.org/10.1038/s41562-020-00959-9.

Ren, Meng, Chunying Zhang, Jiangli Di, Huiqi Chen, Aiqun Huang, John S. Ji, Wannian Liang, et al. 2023. "Exploration of the Preterm Birth Risk-Related Heat Event Thresholds for Pregnant Women: A Population-Based Cohort Study in China." *The Lancet Regional Health - Western Pacific* 37 (August): 100785. https://doi.org/10.1016/j.lanwpc.2023.100785.

Shi, Ying, Zhenyu Han, Ying Xu, and Chan Xiao. 2021. "Impacts of Climate Change on Heating and Cooling Degree-hours Over China." *International Journal of Climatology* 41, no. 3 (March 15, 2021): 1571–1583. https://doi.org/10.1002/joc.6889.

Smith, Caroline J. 2019. "Pediatric Thermoregulation: Considerations in the Face of Global Climate Change." *Nutrients* 11, no. 9 (August 26, 2019): 2010. https://doi.org/10.3390/nu11092010.

Spangler, Keith R., Quinn H. Adams, Jie Kate Hu, Danielle Braun, Kate R. Weinberger, Francesca Dominici, and Gregory A. Wellenius. 2023. "Does Choice of Outdoor Heat Metric Affect Heat-Related Epidemiologic Analyses in the US Medicare Population?" *Environmental Epidemiology* 7, no. 4 (August): e261. https://doi.org/10.1097/EE9.0000000000000261.

Spangler, Keith R., Shixin Liang, and Gregory A. Wellenius. 2022. "Wet-Bulb Globe Temperature, Universal Thermal Climate Index, and Other Heat Metrics for US Counties, 2000–2020." *Scientific Data* 9, no. 1 (June 17, 2022): 326. https://doi.org/10.1038/s41597-022-01405-3.

Sun, Xian, Zhenshan Lin, Xiaoxia Cheng, and Chuangye Jiang. 2008. "Regional Features of the Temperature Trend in China Based on Empirical Mode Decomposition." *Journal of Geographical Sciences* 18, no. 2 (May): 166–176. https://doi.org/10.1007/s11442-008-0166-6.

Sun, Zhiying, Chen Chen, Meilin Yan, Wanying Shi, Jiaonan Wang, Jie Ban, Qinghua Sun, et al. 2020. "Heat Wave Characteristics, Mortality and Effect Modification by Temperature Zones: A Time-Series Study in 130 Counties of China." *International Journal of Epidemiology* 49 (6): 1813–1822. https://doi.org/10.1093/ije/dyaa104.

UNICEF. 2021. "The Climate Crisis is a Child Rights Crisis," August 20, 2021. https://www.unicef.org/reports/climate-crisis-child-rights-crisis.

United Nations Children's Fund. 2022. *The Coldest Year of the Rest of Their Lives: Protecting Children Form the Escalating Impacts of Heatwaves.* New York: UNICEF. https://www.unicef.org/media/129506/file/UNICEF-coldest-year-heatwaves-and-children-EN.pdf.

Wang, Dengjia, Yanchao Xu, Yanfeng Liu, Yingying Wang, Jing Jiang, Xiaowen Wang, and Jiaping Liu. 2018. "Experimental Investigation of the Effect of Indoor Air Temperature on Students' Learning Performance Under the Summer Conditions in China." *Building and Environment* 140 (August): 140–152. https://doi.org/10.1016/j.buildenv.2018.05.022.

Xiao, Xiong, Antonio Gasparrini, Jiao Huang, Qiaohong Liao, Fengfeng Liu, Fei Yin, Hongjie Yu, et al. 2017. "The Exposure-Response Relationship Between Temperature and Childhood Hand, Foot and Mouth Disease: A Multicity Study from Mainland China." *Environment International* 100 (March): 102–109. https://doi.org/10.1016/j.envint.2016.11.021.

Xu, Meimei, Weiwei Yu, Shilu Tong, Lei Jia, Fengchao Liang, and Xiaochuan Pan. 2015. "Non-Linear Association Between Exposure to Ambient Temperature and Children's Hand-Foot-and-Mouth Disease in Beijing, China." Edited by Qinghua Sun. *PLOS ONE* 10, no. 5 (May 26, 2015): e0126171. https://doi.org/10.1371/journal.pone.0126171.

Xu, Zhiwei, Ruth A. Etzel, Hong Su, Cunrui Huang, Yuming Guo, and Shilu Tong. 2012. "Impact of Ambient Temperature on Children's Health: A Systematic Review." *Environmental Research* 117 (August): 120–131. https://doi.org/10.1016/j.envres.2012.07.002.

Yang, Zhou, Jun Yang, Maigeng Zhou, Peng Yin, Zhaoyue Chen, Qi Zhao, Kejia Hu, et al. 2021. "Hourly Temperature Variability and Mortality in 31 Major Chinese Cities: Effect Modification by Individual Characteristics, Season and Temperature Zone." *Environment International* 156 (November): 106746. https://doi.org/10.1016/j.envint.2021.106746.

Zeng, Weilin, Min Yu, Weizhen Mai, Maigeng Zhou, Chunliang Zhou, Yize Xiao, Zhulin Hou, et al. 2022. "Age-Specific Disparity in Life Loss Per Death Attributable to Ambient Temperature: A Nationwide Time-Series Study in China." *Environmental Research* 203 (January): 111834. https://doi.org/10.1016/j.envres.2021.111834.

Zhan, Mingjin, Xiucang Li, Hemin Sun, Jianqing Zhai, Tong Jiang, and Yanjun Wang. 2018. "Changes in Extreme Maximum Temperature Events and Population Exposure in China Under Global Warming Scenarios of 1.5 and 2.0°c: Analysis Using the Regional Climate Model COSMO-CLM." *Journal of Meteorological Research* 32, no. 1 (February): 99–112. https://doi.org/10.1007/s13351-018-7016-y.

Zhang, Wei, Ying Li, Zhuang Li, Xin Wei, Ting Ren, Jie Liu, and Yan Zhu. 2020. "Impacts of Climate Change, Population Growth, and Urbanization on Future Population Exposure to Long-Term Temperature Change During the Warm Season in China." *Environmental Science and Pollution Research* 27, no. 8 (March): 8481–8491. https://doi.org/10.1007/s11356-019-07238-9.

Zhao, Qi, Shanshan Li, Wei Cao, De-Li Liu, Quan Qian, Hongyan Ren, Fan Ding, et al. 2018. "Modeling the Present and Future Incidence of Pediatric Hand, Foot, and Mouth Disease Associated with Ambient Temperature in Mainland China." *Environmental Health Perspectives* 126, no. 4 (April 5, 2018): 047010. https://doi.org/10.1289/EHP3062.

Zivin, Joshua Graff, and Jeffrey Shrader. 2016. "Temperature Extremes, Health, and Human Capital." *The Future of Children* 26 (1): 31–50. https://doi.org/10.1353/foc.2016.0002.

Figure 1: Change in Hourly Temperature Exposure for Children (0-14)

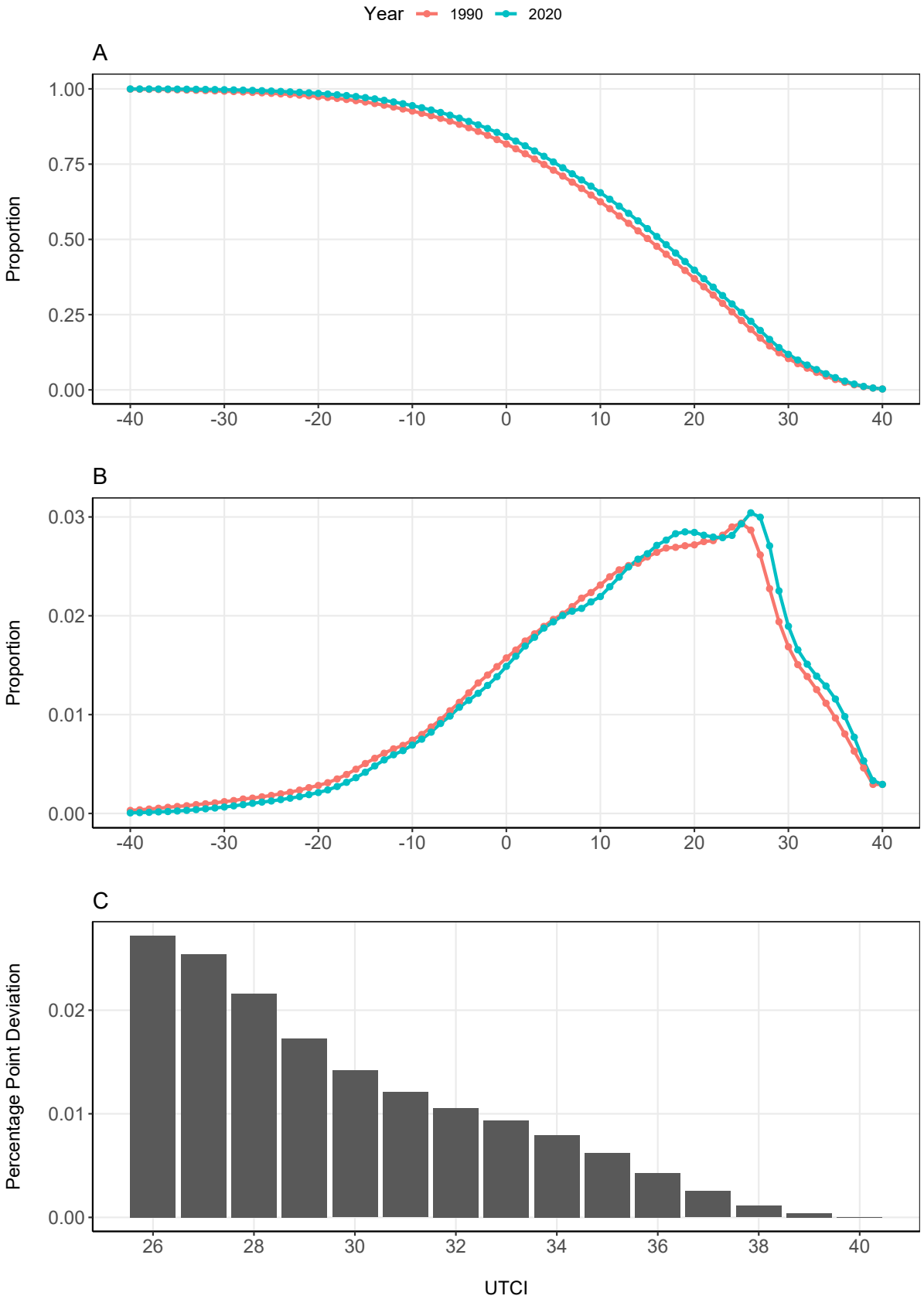

Notes: A. Cumulative Density Curve. B. Probability Density Curve. C. Percentage Point Deviation from 2020 to 1990.

Figure 2: Proportion of Children Experiencing Heat Stress by Proportion of Hours Across Different UTCI Thresholds

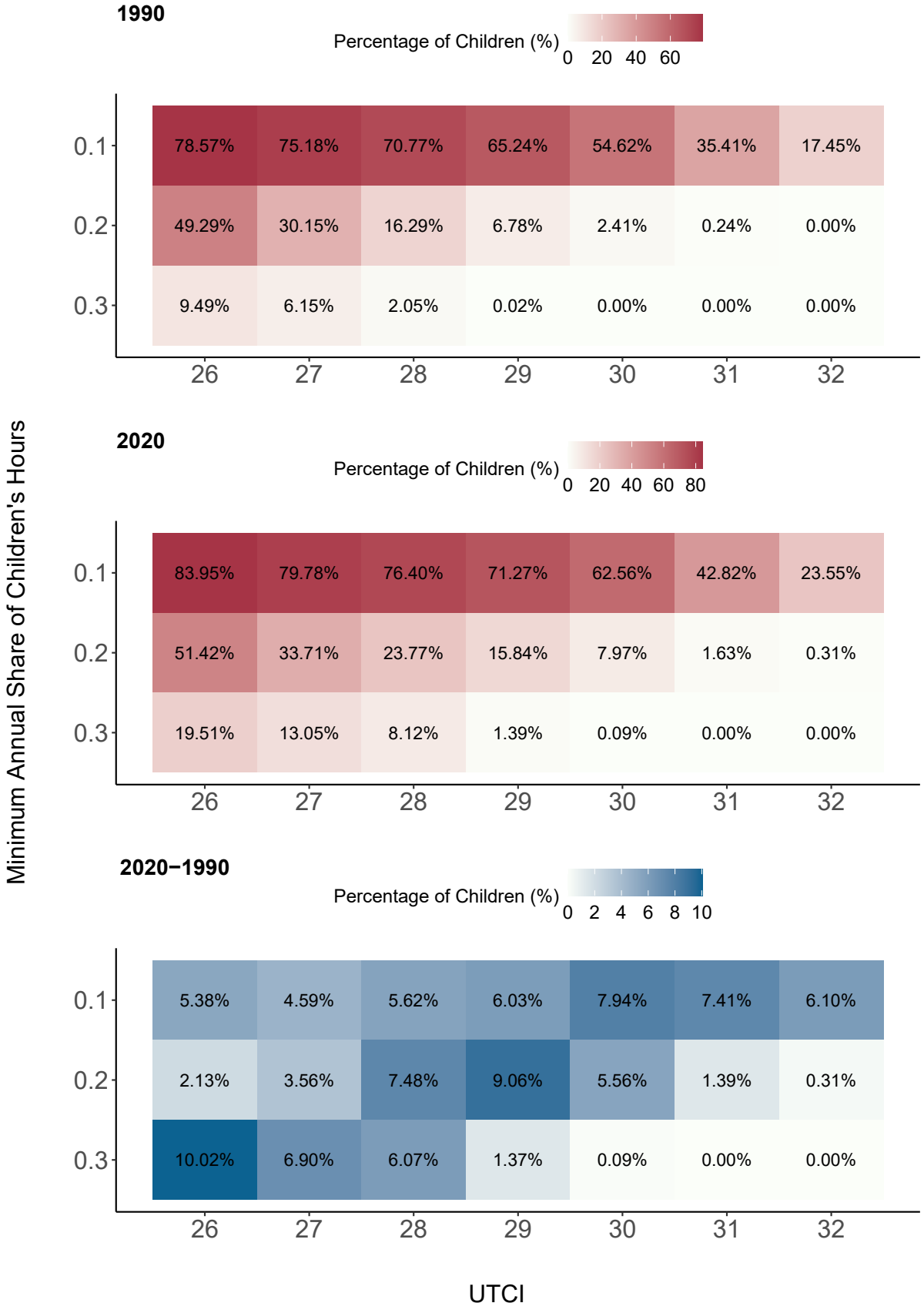

Figure 3: Counterfactual Decomposition Analyses

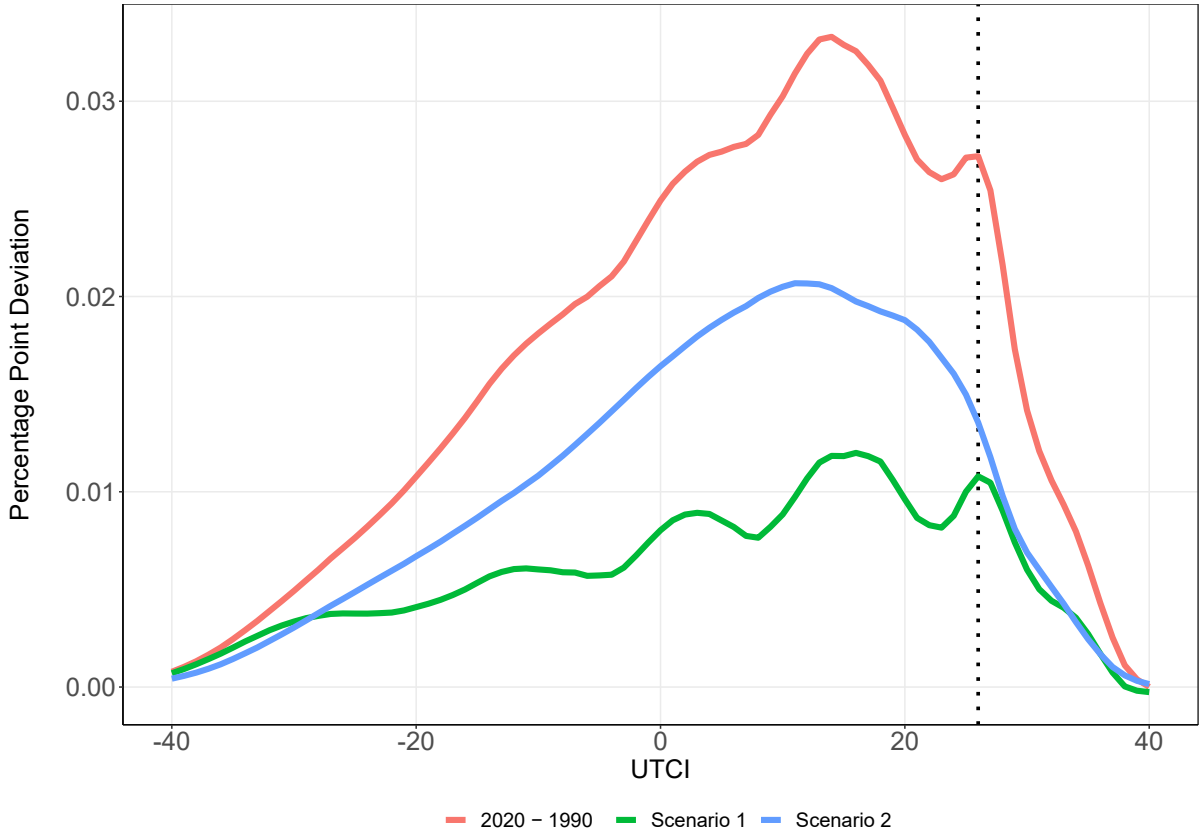

I need to rewrite this to make it clear *Notes*: For all lines, the baseline reference is the children's share of total hour above certain threshold in 1990. The red line represents the percentage difference between children's shares of total hour above certain UTCI threshold and the baseline; In the first counterfactual decomposition, we use children population distribution in 1990 with the observed temperature in 2020. The green line (Scenario 1) represents the percentage difference between the decomposition results with the baseline (climte effect). In the second counterfactual decomposition, we use children population distribution in 2020 with the observed temperature in 1990. The blue line (Scenario 2) represents the percentage difference between the decomposition results with the baseline (population effect).

Figure 4: Regional Differences in UTCI: Ages 0 to 14

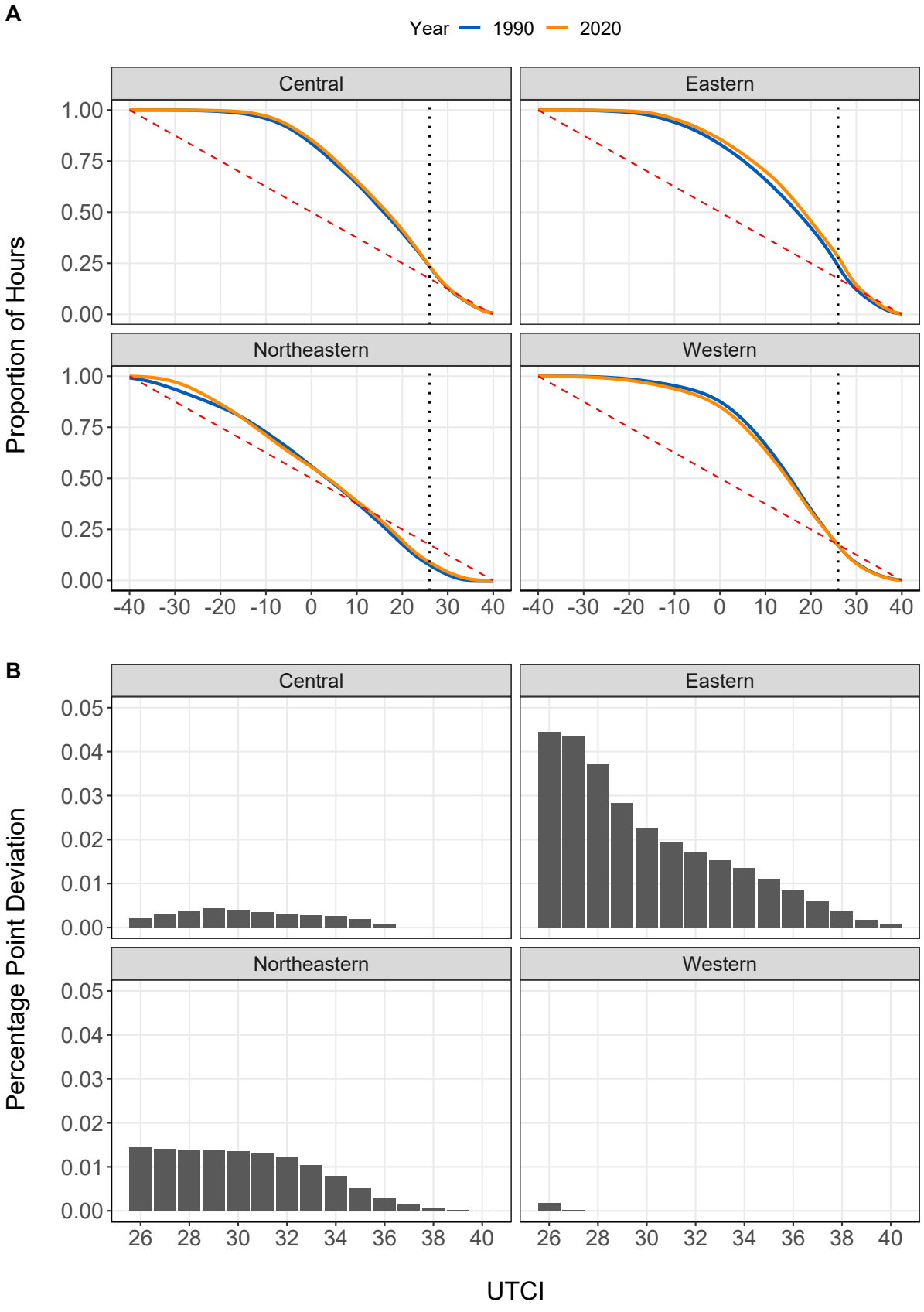

Notes: A. Cumulative Density Curve by Regions. The vertical line indicates 26°C. B. Percentage Point Deviation from 2020 to 1990.

ONLINE APPENDIX

Rising Temperatures, Rising Risks: A Three-Decade Analysis of Children's Heat Exposure in China (1990-2020)

Kai Feng, Marco M. Laghi, Jere R. Behrman, Emily Hannum, and Fan Wang

A Method—Population, Time, and Temperature Exposure

Population, Time, and Temperature Exposure We now formalize our temperature-exposure analysis framework across time and space. Specifically, let $c_l(t)$ be the UTCI temperature experienced by an individual at a moment in time t at a location l. Between period $\underline{t}$ and $\underline{t}+\tau$, the share of time that individuals at location l experience temperature $c_l(t)$ over threshold c^* is, $s_l(c^*, \underline{t}, \tau)$:

$$s_l(c^*, \underline{t}, \tau) = \frac{1}{\tau}\int_{\underline{t}}^{\underline{t}+\tau} \mathbf{1}\{c_l(t) > c^*\}\, dt\ . \tag{1}$$

Additionally, let $P_{\underline{t}\leqslant t<\underline{t}+\tau}(l|m)$ be the share of population for socio-demographic group m in a location l, among L locations in total between time $\underline{t}$ and $\underline{t}+\tau$ where: $\sum_{l=1}^{L} P_{\underline{t}\leqslant t<\underline{t}+\tau}(l|m) = 1$. Meaning that the population m at location l is experiencing exposure.

We compute two key sets of statistics. First, we compute $\mathcal{S}_m(c^*, \underline{t}, \tau)$, which is for a particular interval of time, the average share of time individuals of a socio-demographic group m are exposed to temperature over threshold c^*:

$$\mathcal{S}_m(c^*, \underline{t}, \tau) = \sum_{l=1}^{L} P_{\underline{t}\leqslant t<\underline{t}+\tau}(l|m)\cdot s_l(c^*, \underline{t}, \tau)\,. \tag{2}$$

Since $\mathcal{S}_m(c^*, t, \tau)$ is a share of time, it is between 0 and 1. In particular, $\lim_{c^*\to\infty}\mathcal{S}_m(c^*, t, \tau) = 0$ and $\lim_{c^*\to-\infty}\mathcal{S}_m(c^*, t, \tau) = 1$. A key aggregate statistic for how temperature exposure shifts between period t' and t is the following difference:

$$\Delta\mathcal{S}_{m,t',t}(c^*, \tau) = \mathcal{S}_m\left(c^*, t', \tau\right) - \mathcal{S}_m(c^*, t, \tau)\,. \tag{3}$$

$\Delta\mathcal{S}_{m,t',t}(c^*, \tau)$ is the population-weighted average increase in the share of time exposed to the potential key temperature threshold c^* between time t and t' for population group m. $\Delta\mathcal{S}_{m,t',t}(c^*, \tau)$ shifts due to both shifts in the population distribution as well as the distribu-

tion of temperature between t and t', thus taking into account population and meteorological change.

Second, we compute the share of individuals at risk, based on a joint consideration of the relevant temperature threshold that might be considered risky for human development, and the share of time exposed to such temperature that would put individuals at risk of non-transitory impacts. Our objective here is not to provide what these thresholds should specifically be but to consider, for the first time, these two joint dimensions of risks in computing population-demographic-related exposure statistics. Specifically, let $s^*(\tau)$ be a particular share-of-time threshold within span of time τ above a specific temperature risk threshold. In our analysis, we use an $s^*(\tau)$ of 0.10; 0.20; and 0.30 as shares of time above each UTCI temperature between 26 and 32. We define the m-, c^*-, and s^*-specific at risk measure $\mathcal{R}_m(c^*, s^*, t, \tau)$ between time t and $t+\tau$ as:

$$\mathcal{R}_m(c^*, s^*, \underline{t}, \tau) = \sum_{l=1}^{L} P_{\underline{t} \leqslant t < \underline{t}+\tau}(l|m) \cdot \mathbf{1}\{s_l(c^*, \underline{t}, \tau) > s^*(\tau)\}. \tag{4}$$

By construction, $\mathcal{R}_m(c^*, s^* = 0, t, \tau) \leqslant 1$ and $\mathcal{R}_m(c^*, s^* = 1, t, \tau) = 0$. Additionally, the share of individuals experiencing greater than s^* share of time over c^* threshold converges to 0 as c^* increases: $\lim_{c^* \to \infty} \mathcal{R}_m(c^*, s^*, t, \tau) = 0$.

For the socio-demographic group indexed by m, given temperature threshold c^* and share of time threshold s^*, the percentage increase over time in the share of individuals from this group at risk of excess heat exposure is:

$$\Delta\mathcal{R}_{m,t',t}(c^*, s^*, \tau) = \mathcal{R}_m\left(c^*, s^*, t', \tau\right) - \mathcal{R}_m(c^*, s^*, t, \tau). \tag{5}$$

In our empirical application t is 1990 and, t' is 2020, τ is one calendar year, and m is children between age 0 to 14. Additionally, we approximate continuous time with hourly measurements. As an example, $\Delta\mathcal{R}_{\text{children},2020,1990}$ with $c^* = 28$ and $s^* = 0.1$ provides the change in the percentage points of children exposed to temperature over 28 degrees for greater than 10 percent of their time during a year.

One important aspect of our framework is that computing $\mathcal{R}_m(c^*, s^*, t, \tau)$ and $\Delta\mathcal{R}_{m,t',t}(c^*, s^*, \tau)$ do not require the use of harmonized geographic data overtime. This is often a constraint in the analysis of temperature changes over time, due to shifting boundaries of administrative boundaries, especially across large spans of time. In our analysis, the unit of interest is m, the

socio-demographic group; at times t and t', thus the geographical boundaries can shift.

Existing literature A large number of papers focused on climatic changes across locations compute location-specific means between times $\underline{t}$ and $\underline{t}+\tau$, and use $E_{l,\underline{t},\tau}$ for comparison across locations:

$$E_{l,\underline{t},\tau}(c) = \frac{1}{\tau}\int_{\underline{t}}^{\underline{t}+\tau} c_l(t)\,dt\ . \tag{6}$$

Additionally, by dividing the interval of time τ into M sub-periods (e.g., days), some paper focus on analyzing the averages of minimum and maximum. Specifically, given M sub-periods, $E^{max}_{l,\underline{t},\tau,M}$ is the average of sub-period-specific maximum temperature between $\underline{t}$ and $\underline{t}+\tau$:

$$E^{max}_{l,\underline{t},\tau,M} = \sum_{m=1}^{M}\frac{1}{M}\max\left(c_l(t)\cdot\mathbb{1}\left(\underline{t}+\frac{\tau}{M}\cdot(m-1)\leqslant t<\frac{\tau}{M}\cdot(m)\right)\right)\ . \tag{7}$$

And $E^{min}_{l,\underline{t},\tau,M}$ is the average of the sub-period-specific minima:

$$E^{min}_{l,\underline{t},\tau,M} = \sum_{m=1}^{M}\frac{1}{M}\max\left(c_l(t)\cdot\mathbb{1}\left(\underline{t}+\frac{\tau}{M}\cdot(m-1)\leqslant t<\frac{\tau}{M}\cdot(m)\right)\right)\ . \tag{8}$$

Various papers in the existing scientific literature focus on comparing these statistics over time between period t and t' to study changes in climatic conditions across time for different locations.

In the social science literature, the focus has been on estimating the effects of temperature exposures $E^{mean}_{l,\underline{t},\tau}$, $E^{max}_{l,\underline{t},\tau,M}$, $E^{min}_{l,\underline{t},\tau,M}$ on outcomes related to human capacities ranging from educational attainment, health outcomes, to productivity outcomes.

Rather than using $c_l(t)$ directly, a subset of the literature in social science computes the above mentioned statistics with $c^z_l(t)$, which are based on location-specific deviations from prior trends, sometimes computed in standard deviation units, for example: $c^z_l(t) = \frac{E^{mean}_{l,t,\tau} - E^{mean}_{l,t^*,\tau^*}}{\sqrt{VAR_{l,t^*,\tau^*}}}$

B Data

B.1 ERA5 Data Details

ERA5-HEAT, produced by the European Centre for Medium-Range Weather Forecasts (ECMWF), represents the fifth generation of atmospheric reanalyses of global climate (Napoli 2020). Covering the period from 1979 to the present, ERA5-HEAT comprises hourly gridded maps of Universal Thermal Climate Index (UTCI) at 0.25° × 0.25° spatial resolution. The dataset is publicly accessible through the Copernicus Climate Change Service's Climate Data Store (CDS).

For standard geo-based analysis over time, a key stumbling block is harmonizing location boundaries that may change over time. This is normally difficult to deal with when we have county-level boundaries, as Chinese administrative names and boundaries have changed substantially over 30 years. Luckily, we are not necessarily trying to compare a county to its own borders across 30 years, instead, we compare similarly fine and consistent measures of population and temperature distribution across time that in this case match well with county boundaries. Another option might be to proceed is via the use of prefecture data in 1990 and county data in 2020, but that might not be as appropriate or easily interpretable.

As described by Bröde et al. (2012), Jendritzky, Dear, and Havenith (2012), and Jendritzky and Höppe (2017), the UTCI is a widely used index to assess the human-perceived environment based on atmospheric conditions, integrating atmospheric parameters like temperature, humidity, wind speed, and solar radiation. UTCI is expressed in degrees Celsius (°C), and it provides a measure of how cold or hot people might feel under prevailing environmental conditions. The index categorizes thermal stress into different classes with corresponding thresholds, which are as follows:

Extreme cold stress: UTCI below -40°C; Very strong cold stress: UTCI -40°C to -27°C; Strong cold stress: UTCI -27°C to -13°C; Moderate cold stress: UTCI -13°C to 0°C; No thermal stress: UTCI 0°C to 26°C; Moderate heat stress: UTCI 26°C to 32°C; Strong heat stress: UTCI 32°C to 38°C; Very strong heat stress: UTCI 38°C to 46°C; Extreme heat stress: UTCI above 46°C;

B.2 Population data input specification

In each census year, we determine the population distribution by dividing the population of each age and gender group in each county by the entire population in the census year. For our analysis of children's exposure, we focus on the age group between 0 to 14 regardless of

gender.

Census 1990 We obtained 2369 geographical units at the county level nested in 31 provincial administrative regions from the Tabulation on 1990 China Population Census by County. We start with the 1990 Chinese Census as it is the first to offer county-level population counts by ages 0-14. We only include mainland China and did not include special administrative regions. Within each county, we have population data by gender and age.

Census 2020 We obtained 2853 geographical units at the county level nested in 31 provincial administrative regions from the Tabulation on 2020 China Population Census by County. We only include mainland China and did not include special administrative regions. Within each county, we have population data by gender and age.

C Method Data Framework

C.1 ERA5-HEAT data input specification

We use the thermal comfort index, UTCI, derived from ERA5 reanalysis. This data, ERA5-HEAT, is publicly accessible through the Climate Data Store API service from the European Centre for Medium-Range Weather Forecasts. The ERA5-HEAT dataset provides hourly UTCI from January 1940 to near real-time in 0.25° by 0.25° (roughly 31 kilometers) latitude-longitude grid in NetCDF format.

In order to capture the entire China mainland area, we employ China's far-east (135°E), far-west (53°E), far-south (4°N), and far-north (54°N) points as spatial references in our API request to extract a rectangle area that contains gridded points with latitude and longitude coordinates from the ERA5-HEAT data. For the time periods, We specify all months and dates in census year 1990, 2000, 2010, 2020 respectively in our API request. After having coordinate-specific hourly UTCI from all dates, we consolidate them into one data file by year. For example, in the 2020 data file, each coordinate in the gridded map includes hourly UTCI values from January 1, 2020 to December 31, 2020.

C.2 Population data input specification

We obtain county-level demographic data from the census tabulations. In each census file, there is one unique identification number for each county. Each county includes demographic data by age group and gender for the corresponding census year. The county shapefiles provide the geometry defining the boundaries of each county. This geometry is important for linking the population data with the gridded UTCI data.

The final population input consists of a data matrix. In this matrix, one column signifies a distinct county ID, while each row denotes the proportion of the population by gender within specific 5-year age groups (ranging from 0-4 to 85+) relative to the total population of one census year. The heat exposure and share of children at risk are constructed considering only the age groups of 0-4, 5-9, and 10-14, combining data for both males and females. However, our approach has the flexibility to extend to any demographic group as needed.

C.3 Specifying key files

There are three key files (1) key file that links the coordinate to county. (2) key file that links county to province and regions. (3) key file that links population input column variables to the original labels (e.g., age groups and gender), and grouping variables for aggregation purposes (i.e., age groups 0-14, 15-64, 65+).

We obtain the geography boundary for each county from the census shapefile. Note that the county boundary may change from census to census. We had 2853 counties in 2020 and we had 2369 counties in 1990. We identify the grid coordinates from ERA5-HEAT that fall within the county boundary. In each census year, we create a key file that includes a unique identification number for each county, and all the coordinates within the county boundary. This key file helps us to merge the ERA5-HEAT data with the county-level census data.

D Additional Results on heat exposure for children

D.1 Average shares of time of heat exposure for children

In Tables D.1 and D.2, we present additional details on changes in average heat exposure between 1990 and 2020 for Chinese children (ages 0–14). We focus on the annual average share of time that Chinese children are exposed to UTCI temperature over thresholds $z\,^{\circ}$C. We group thresholds into four panels focusing at exposures to at least borderline thermal stress (23 °C–25 °C), to at least moderate heat stress (26 °C–31 °C), to at least strong heat stress (32 °C–37 °C), and to different thresholds of very strong heat exposure (38 °C–40 °C).

Table D.1's first four columns contain our main results where we consider ambient exposure during all hours of 1990 and 2020. The remaining four columns in Table D.1 present results considering only day time (between 6 am and 10 am) hours. Table D.2 presents results where we compare heat exposure in the warmer months of April, May, June, July, August and September with heat exposure in the colder months of January, February, March, October, November and December in 1990 and 2020.

EDIT PLEASE: *Discuss briefly additional details here, consider changes to main text, ideas*

1. Share of time with **at least** moderate, strong, very strong heat stress all increasing

2. Note for the 2.7 pp of increase in heat exposure $\geqslant 26\,^{\circ}$C, that is not all due to increases in moderate heat stress. We see that there is 1.1 pp increase in heat exposure $\geqslant 32\,^{\circ}$C. Jointly these mean that approximately 60% $\left(\frac{2.7-1.1}{2.7} \approx 0.6\right)$ of the 2.7 pp comes from increases in moderate heat exposure.

3. Approximately 30 to 50 percent higher share of time exposed in 2020 for day time vs all day hours, a mechanical result, due to us dropping about 40 percent of the hours from the day $((24-14)/24)$.

4. Between 14 and 18 percentage increases in exposure under panel B and C for all hours, day time only, as well as April-September results. October to March started with very low levels in 1990 of average very strong and at least strong heat exposures, and experienced very large percentage increases.

Table D.1: Changes in average share of time exposed to heat

	All annual hours ⩾ UTCI thresholds				Day time (6 am-10 pm) hours ⩾ UTCI thresholds			
	Share of time		Changes		Share of time		Changes	
UTCI thresholds	1990	2020	Level	%	1990	2020	Level	%
Panel A: Very strong heat stress								
⩾ 40 °C	0.3%	0.3%	0.0007pp	0.2%	0.4%	0.4%	0.001pp	0.2%
⩾ 39 °C	0.6%	0.6%	0.0pp	6.7%	0.9%	0.9%	0.1pp	6.7%
⩾ 38 °C	1.0%	1.2%	0.1pp	10.6%	1.6%	1.7%	0.2pp	10.7%
Panel B: At least strong heat stress								
⩾ 37 °C	1.7%	1.9%	0.3pp	15.1%	2.5%	2.9%	0.4pp	15.1%
⩾ 36 °C	2.5%	2.9%	0.4pp	17.3%	3.7%	4.4%	0.6pp	17.3%
⩾ 35 °C	3.4%	4.1%	0.6pp	18.1%	5.2%	6.1%	0.9pp	18.1%
⩾ 34 °C	4.6%	5.4%	0.8pp	17.5%	6.8%	8.0%	1.2pp	17.5%
⩾ 33 °C	5.8%	6.7%	0.9pp	16.1%	8.7%	10.1%	1.4pp	16.1%
⩾ 32 °C	7.2%	8.3%	1.1pp	14.7%	10.8%	12.3%	1.6pp	14.8%
Panel C: At least moderate heat stress								
⩾ 31 °C	8.7%	9.9%	1.2pp	13.9%	12.9%	14.7%	1.8pp	13.8%
⩾ 30 °C	10.4%	11.8%	1.4pp	13.6%	15.2%	17.3%	2.0pp	13.2%
⩾ 29 °C	12.3%	14.1%	1.7pp	14.0%	17.7%	20.0%	2.3pp	12.8%
⩾ 28 °C	14.6%	16.8%	2.2pp	14.8%	20.4%	22.9%	2.6pp	12.5%
⩾ 27 °C	17.2%	19.8%	2.5pp	14.8%	23.2%	26.0%	2.8pp	12.0%
⩾ 26 °C	20.1%	22.8%	2.7pp	13.5%	26.2%	29.1%	2.9pp	11.0%
Panel D: At least borderline thermal stress								
⩾ 25 °C	23.0%	25.7%	2.7pp	11.8%	29.3%	32.1%	2.8pp	9.7%
⩾ 24 °C	25.9%	28.6%	2.6pp	10.1%	32.3%	35.1%	2.7pp	8.5%
⩾ 23 °C	28.7%	31.3%	2.6pp	9.0%	35.3%	38.1%	2.7pp	7.7%

Note: Columns 1, 2, 5, and 6 show the annual average shares of time that children in China (ages 0–14) are exposed to UTCI temperatures at ⩾ z °C. Columns 3, 4, 7, and 8 show 1990 to 2020 changes in percentage points (level) or percentage (%) of the average shares of time exposed to heat. We consider both all hourly as well as only day time (between 6 am and 10 am) temperatures data.

Table D.2: Changes in average share of time exposed to heat during warmer and colder months

	April–September hours ⩾ UTCI thresholds				October–March hours ⩾ UTCI thresholds			
	Share of time		Changes		Share of time		Changes	
UTCI thresholds	1990	2020	Level	%	1990	2020	Level	%
Panel A: Very strong heat stress								
⩾ 40 °C	0.6%	0.6%	0.001pp	0.2%	0.00002%	0.00008%	0.00006pp	334.3%
⩾ 39 °C	1.2%	1.2%	0.1pp	6.6%	0.0001%	0.0004%	0.0002pp	159.0%
⩾ 38 °C	2.1%	2.3%	0.2pp	10.6%	0.0004%	0.002%	0.001pp	373.7%
Panel B: At least strong heat stress								
⩾ 37 °C	3.3%	3.8%	0.5pp	14.9%	0.002%	0.010%	0.008pp	476.0%
⩾ 36 °C	4.9%	5.8%	0.8pp	17.0%	0.006%	0.02%	0.0pp	291.4%
⩾ 35 °C	6.9%	8.1%	1.2pp	17.7%	0.02%	0.05%	0.0pp	144.1%
⩾ 34 °C	9.0%	10.6%	1.6pp	17.1%	0.06%	0.10%	0.0pp	67.0%
⩾ 33 °C	11.5%	13.3%	1.8pp	15.8%	0.1%	0.2%	0.0pp	35.1%
⩾ 32 °C	14.1%	16.2%	2.1pp	14.7%	0.3%	0.3%	0.0pp	14.1%
Panel C: At least moderate heat stress								
⩾ 31 °C	16.9%	19.3%	2.4pp	14.2%	0.5%	0.5%	0.0pp	4.2%
⩾ 30 °C	20.0%	22.8%	2.8pp	14.1%	0.8%	0.8%	0.0pp	2.5%
⩾ 29 °C	23.4%	26.9%	3.4pp	14.6%	1.2%	1.2%	0.0pp	3.0%
⩾ 28 °C	27.5%	31.7%	4.3pp	15.5%	1.7%	1.7%	0.1pp	3.4%
⩾ 27 °C	32.0%	37.0%	5.0pp	15.6%	2.4%	2.4%	0.1pp	2.8%
⩾ 26 °C	36.9%	42.2%	5.3pp	14.5%	3.2%	3.3%	0.1pp	2.5%
Panel D: At least borderline thermal stress								
⩾ 25 °C	41.7%	47.0%	5.3pp	12.7%	4.2%	4.4%	0.1pp	2.7%
⩾ 24 °C	46.3%	51.4%	5.1pp	11.0%	5.4%	5.6%	0.2pp	3.0%
⩾ 23 °C	50.6%	55.5%	4.9pp	9.7%	6.8%	7.1%	0.3pp	4.0%

Note: Columns 1, 2, 5, and 6 show the annual average shares of time that children in China (ages 0–14) are exposed to UTCI temperatures at ⩾ z °C. Columns 3, 4, 7, and 8 show 1990 to 2020 changes in percentage points (level) or percentage (%) of the average shares of time exposed to heat. We compare temperatures across time for April, May, June, July, August and September and then for January, February, March, October, November and December of each year. We consider all 24 hours.

D.2 Share of children at risk of heat exposure

In Tables D.3 and D.4, we present additional details from the analysis of the share of children at risk of heat exposure, considering the double thresholds of intensity (UTCI temperature thresholds z °C) and duration (share of time in year thresholds y%). In each scenario, the share of children is computed by aggregating the share of child population from locations (counties) experiencing these double thresholds of exposures.

In both Tables D.3 and D.4, across the columns, we present 9 duration thresholds, starting with at least half a month or 2 weeks of heat exposure (approximately 4% of a year's time) and ending with at least 3.5 months or 18 weeks (approximately 36% of a year's time) of exposure. Across the rows, we consider UTCI thresholds including a number of at least moderate and at least strong heat stress thresholds. In Table D.3, Panels A and B present shares of children at risk in 1990 and 2020. In Table D.3, Panels A and B present percentage points and percentage changes between 1990 and 2020.

EDIT PLEASE: *Discuss briefly additional details here, consider changes to main text, ideas*

1. **Universal low exposure**: 97% and 70% of children experience at least 2 weeks or half a month of at least moderate heat stress ($\geqslant 26\,^{\circ}$C) and at least strong heat stress ($\geqslant 32\,^{\circ}$C)

2. **Very strong heat, increase in intensity**: Less than 0.05% of children experienced very strong heat ($\geqslant 38\,^{\circ}$C) stress in 1980 (below threshold for showing up in the tables), but in 2020, 0.7% (0.1%) of children (not a small number) are exposed for at least 2 weeks (4 weeks) to ambient very strong heat stress.

3. **Strong heat, increases in duration**: very large increases in shares of children experiencing longer aggregate shares of time under at least strong heat stress ($\geqslant 32\,^{\circ}$C, $\geqslant 34\,^{\circ}$C, $\geqslant 36\,^{\circ}$C). Share of children experiencing at least 2 months of at least strong heat stress ($\geqslant 32\,^{\circ}$C) nearly quadruples from 1.1% to 4.1% of children.

4. **Moderate heat, very long duration**: At the tail, 6.5% of children experienced at least 3.5 months of at least moderate heat stress ($\geqslant 26\,^{\circ}$C) in 1990, this doubled to 13.5% of children in 2020. 3.2% of children experienced at least 2.5 months of at least moderate heat stress ($\geqslant 30\,^{\circ}$C) in 1990, this triples to 9.1% of children in 2020.

Table D.3: Minimal shares of children (ages 0–14) at risk of heat exposure

	Minimal share of time in year thresholds and corresponding number of weeks								
	$\geqslant 4\%$	$\geqslant 8\%$	$\geqslant 12\%$	$\geqslant 16\%$	$\geqslant 20\%$	$\geqslant 24\%$	$\geqslant 28\%$	$\geqslant 32\%$	$\geqslant 36\%$
UTCI thresholds	2 weeks	4 weeks	6 weeks	8 weeks	10 wks	12 wks	14 wks	16 wks	18 wks
Panel A: 1990									
x% (cell) of children with at least y% (column) of time in year 1990 at $\geqslant z$ °C (row) heat threshold									
Very strong heat stress									
$\geqslant 38$ °C									
At least strong heat stress									
$\geqslant 36$ °C	20.3%	0.1%							
$\geqslant 34$ °C	56.7%	10.4%	0.2%						
$\geqslant 32$ °C	70.7%	46.8%	7.4%	1.1%					
At least moderate heat stress									
$\geqslant 30$ °C	79.6%	67.9%	37.4%	11.1%	3.2%	0.2%			
$\geqslant 28$ °C	89.3%	76.5%	66.7%	40.0%	18.1%	6.7%	3.7%	1.2%	
$\geqslant 26$ °C	96.5%	85.3%	75.7%	67.3%	51.8%	29.0%	15.3%	8.5%	6.5%
At least borderline thermal stress									
$\geqslant 24$ °C	98.5%	94.6%	83.6%	75.9%	69.7%	61.4%	41.3%	23.3%	13.2%
Panel B: 2020									
x% (cell) of children with at least y% (column) of time in year 2020 at $\geqslant z$ °C (row) heat threshold									
Very strong heat stress									
$\geqslant 38$ °C	0.7%	0.1%							
At least strong heat stress									
$\geqslant 36$ °C	22.4%	1.4%	0.1%						
$\geqslant 34$ °C	63.7%	17.4%	2.0%	0.3%					
$\geqslant 32$ °C	76.3%	54.2%	17.2%	4.1%	0.6%				
At least moderate heat stress									
$\geqslant 30$ °C	84.6%	73.2%	46.7%	18.9%	9.1%	1.8%	0.4%		
$\geqslant 28$ °C	93.3%	81.7%	72.7%	47.3%	24.7%	16.4%	10.3%	6.9%	3.3%
$\geqslant 26$ °C	97.4%	90.2%	80.4%	73.3%	54.4%	33.6%	24.1%	17.2%	13.5%
At least borderline thermal stress									
$\geqslant 24$ °C	98.6%	96.6%	88.3%	80.6%	75.6%	63.2%	42.4%	31.3%	22.7%

Note: Cells show the shares of Chinese children (ages 0–14) experiencing at least y% of their time in a year over a particular z °C UTCI temperature threshold. Shares of children at risk are computed based on aggregating population shares from locations (counties) experiencing the various combinations of heat stress duration (share of time) and intensity (temperature) thresholds. For minimal shares of time in year, the correspondence between share of time and number of weeks is based on the fact that the average of N weeks of time and $\frac{N}{4}$ months of time is approximately $(N \cdot 2)\%$ of total share of time in a year. To enhance contrast, values are rounded and cells with values less than 0.05% or 0.05pp are left empty. We consider all 24 hours and 12 months.

Table D.4: Changes in shares of children (ages 0–14) at risk of heat exposure

	Minimal share of time in year thresholds and corresponding number of weeks								
	$\geqslant$ 4%	$\geqslant$ 8%	$\geqslant$ 12%	$\geqslant$ 16%	$\geqslant$ 20%	$\geqslant$ 24%	$\geqslant$ 28%	$\geqslant$ 32%	$\geqslant$ 36%
UTCI thresholds	2 weeks	4 weeks	6 weeks	8 weeks	10 wks	12 wks	14 wks	16 wks	18 wks
Panel A: 2020% − 1990%									
Increases in percentage points (cell) of children with at least y% (column) of time at $\geqslant z$ °C (row) heat threshold									
Very strong heat stress									
$\geqslant$ 38 °C	0.7pp	0.1pp							
At least strong heat stress									
$\geqslant$ 36 °C	2.1pp	1.4pp	0.1pp						
$\geqslant$ 34 °C	7.0pp	7.0pp	1.8pp	0.3pp					
$\geqslant$ 32 °C	5.6pp	7.4pp	9.8pp	3.0pp	0.5pp				
At least moderate heat stress									
$\geqslant$ 30 °C	5.1pp	5.3pp	9.3pp	7.8pp	5.9pp	1.6pp	0.4pp		
$\geqslant$ 28 °C	4.0pp	5.1pp	6.0pp	7.3pp	6.5pp	9.7pp	6.6pp	5.8pp	3.3pp
$\geqslant$ 26 °C	0.9pp	5.0pp	4.8pp	6.0pp	2.6pp	4.6pp	8.7pp	8.7pp	7.0pp
At least borderline thermal stress									
$\geqslant$ 24 °C	0.1pp	2.0pp	4.7pp	4.6pp	5.9pp	1.8pp	1.1pp	8.1pp	9.5pp
Panel B: $\frac{2020\% - 1990\%}{1990\%} \cdot 100$									
Percentage increases (cell) of children with at least y% (column) of time at $\geqslant z$ °C (row) heat threshold									
Very strong heat stress									
$\geqslant$ 38 °C									
At least strong heat stress									
$\geqslant$ 36 °C	10.5%	1.6k%							
$\geqslant$ 34 °C	12.3%	66.9%	907%						
$\geqslant$ 32 °C	7.9%	15.7%	132%	273%	1.3k%				
At least Moderate heat stress									
$\geqslant$ 30 °C	6.4%	7.9%	24.8%	70.9%	181%	681%			
$\geqslant$ 28 °C	4.5%	6.7%	9.0%	18.2%	36.0%	144%	179%	499%	8.0k%
$\geqslant$ 26 °C	0.9%	5.8%	6.3%	8.9%	5.1%	16.0%	56.9%	103%	108%
At least borderline thermal stress									
$\geqslant$ 24 °C	0.1%	2.1%	5.6%	6.1%	8.4%	2.9%	2.7%	34.8%	72.3%

Note: Cells show changes between 1990 and 2020 in percentage points (Panel A) and percentage (Panel B) of the shares of Chinese children (ages 0–14) experiencing at least y% of their time in a year over a particular z °C UTCI temperature threshold. Shares of children at risk are computed based on aggregating population shares from locations (counties) experiencing the various combinations of heat stress duration (share of time) and intensity (temperature) thresholds. For minimal shares of time in year, the correspondence between share of time and number of weeks is based on the fact that the average of N weeks of time and $\frac{N}{4}$ months of time is approximately $(N \cdot 2)$% of total share of time in a year. To enhance contrast, values are rounded and cells with values less than 0.05% or 0.05pp are left empty. We consider all 24 hours and 12 months.

D.3 Decomposition shifting only population or temperature distributions

In this section, we provide more details on the relative contributions of shifts in the child population distribution and the temperature distribution to overall changes in average share time exposed to heat. Our decomposition analysis is statistical: we shift one distribution while holding the other constant and do not model mechanisms of changes. Also note that actual changes unexplained by the sum of population and temperature decompositions are attributable to population and temperature interactions.

Following Table D.1, columns 1–3 of Table D.5 include actual annual average shares of time that children are exposed to UTCI temperatures at $\geqslant z$ °C and percentage points changes over time. In columns 4–6, we compute exposures using the 1990 population distribution jointly with the 2020 UTCI temperature distribution. In columns 7–9, we consider exposures if the 2020 population distribution faced the 1990 UTCI temperature distribution. We present in Panel A national results. Panels B and C show results in the eastern and northeastern regions which experienced large increases heat exposure (see Tables D.6 and D.6).

EDIT PLEASE: *Discuss briefly additional details here, consider changes to main text, ideas*

1. **Nationally and regionally, shifts in population matters**: For at least strong ($\geqslant$ 32 °C) and at least moderate heat ($\geqslant$ 26 °C) stress levels, child population distribution shifts nationally (in eastern/northeaster regions) account for 48% (29%/9%) and 50% (38%/16%) of the actual change, respectively. In contrast, temperature distribution shifts account for 42% (61%/92%) and 40% (51%/81%) of the actual changes, respectively.

2. **Cross-regional movements matters**: National, eastern (10 provincial units), and northeastern (3 provincial units) population shifts account approximately 1/2, 1/3, and less than 1/5 of the actual shifts in their respective geographies. The national results are due to shifts within and across regions.

3. **Shifts in population matters less at higher UTCI thresholds**: Contribution of population distribution decreases with increasing heat stress thresholds—nationally (in eastern/northeaster regions) from 61% (53%/20%) at $\geqslant$ 24 °C to 39% (19%/5%) at $\geqslant$ 36 °C. Increases in the higher heat exposures come more from increasing temperatures rather than from population moving to locations that were already hotter in 1990.

Table D.5: Decompose changes in average share of time exposed to heat

	Actual 2020 vs 1990			2020 UTCI with 1990 population			1990 UTCI with 2020 population		
	Share of time		Changes	Share-time	Decompose changes		Share-time	Decompose changes	
UTCI thresholds	1990	2020	Δ	Prediction	Vs. 1990	% of Δ	Prediction	Vs. 1990	% of Δ
Panel A: National									
At least strong heat stress									
$\geqslant 36\,^{\circ}C$	2.5%	2.9%	0.43pp	2.7%	0.17pp	40%	2.7%	0.17pp	39%
$\geqslant 34\,^{\circ}C$	4.6%	5.4%	0.80pp	4.9%	0.35pp	45%	4.9%	0.33pp	42%
$\geqslant 32\,^{\circ}C$	7.2%	8.3%	1.06pp	7.6%	0.44pp	42%	7.7%	0.51pp	48%
At least moderate heat stress									
$\geqslant 30\,^{\circ}C$	10.4%	11.8%	1.42pp	11.0%	0.60pp	42%	11.1%	0.69pp	49%
$\geqslant 28\,^{\circ}C$	14.6%	16.8%	2.16pp	15.5%	0.90pp	42%	15.6%	0.98pp	45%
$\geqslant 26\,^{\circ}C$	20.1%	22.8%	2.72pp	21.2%	1.08pp	40%	21.4%	1.35pp	50%
At least borderline thermal stress									
$\geqslant 24\,^{\circ}C$	25.9%	28.6%	2.63pp	26.8%	0.88pp	33%	27.5%	1.60pp	61%
Panel B: Eastern region									
At least strong heat stress									
$\geqslant 36\,^{\circ}C$	2.7%	3.5%	0.85pp	3.3%	0.59pp	70%	2.9%	0.16pp	19%
$\geqslant 34\,^{\circ}C$	5.3%	6.6%	1.35pp	6.1%	0.89pp	66%	5.6%	0.31pp	23%
$\geqslant 32\,^{\circ}C$	8.4%	10.1%	1.70pp	9.5%	1.03pp	61%	8.9%	0.50pp	29%
At least moderate heat stress									
$\geqslant 30\,^{\circ}C$	12.1%	14.3%	2.26pp	13.4%	1.33pp	59%	12.8%	0.73pp	32%
$\geqslant 28\,^{\circ}C$	17.0%	20.7%	3.70pp	19.0%	2.02pp	55%	18.2%	1.18pp	32%
$\geqslant 26\,^{\circ}C$	23.6%	28.1%	4.44pp	25.9%	2.27pp	51%	25.3%	1.69pp	38%
At least borderline thermal stress									
$\geqslant 24\,^{\circ}C$	30.6%	34.2%	3.54pp	32.0%	1.36pp	38%	32.5%	1.87pp	53%
Panel C: Northeastern region									
At least strong heat stress									
$\geqslant 36\,^{\circ}C$	0.04%	0.3%	0.27pp	0.3%	0.24pp	89%	0.05%	0.01pp	5%
$\geqslant 34\,^{\circ}C$	0.3%	1.1%	0.79pp	1.%	0.72pp	91%	0.3%	0.05pp	6%
$\geqslant 32\,^{\circ}C$	1.1%	2.4%	1.22pp	2.3%	1.12pp	92%	1.3%	0.11pp	9%
At least moderate heat stress									
$\geqslant 30\,^{\circ}C$	2.8%	4.1%	1.35pp	4.0%	1.23pp	91%	2.9%	0.17pp	13%
$\geqslant 28\,^{\circ}C$	5.0%	6.4%	1.39pp	6.2%	1.21pp	87%	5.2%	0.21pp	15%
$\geqslant 26\,^{\circ}C$	7.5%	8.9%	1.43pp	8.7%	1.16pp	81%	7.7%	0.24pp	16%
At least borderline thermal stress									
$\geqslant 24\,^{\circ}C$	10.4%	11.8%	1.45pp	11.4%	1.06pp	73%	10.7%	0.29pp	20%

Note: Columns (cols) 1–3 include actual annual average shares of time that children in China (ages 0–14) are exposed to UTCI temperatures at $\geqslant z\,^{\circ}C$ (same information as cols 1–3 in Table D.1). Cols 4–6 consider heat exposure if the 1990 population distribution faced the 2020 UTCI temperature distribution. Cols 7–9 consider exposure if 2020 population faced 1990 UTCI temperatures. Cols 4 and 7 show predictions of annual average shares of time exposed to heat thresholds given decomposition scenarios. Cols 5 and 8 show differences between predictions and 1990 actual average shares. Cols 6 and 9 show share of column 3 actual changes that predictions from cols 5 and 8 account for. See Table D.6 for provincial level administrative units in the eastern and northeastern regions. We consider all 24 hours and 12 months.

D.4 Additional regional analysis

In this section, we augment the region-specific heat exposure analysis with province-specific analysis as well. Similar to Table D.6, we analyze changes in average heat exposure between 1990 and 2020 for Chinese children. Overall national, regional or provincial changes are due to shifts over time in both the temperature distribution and the child population distribution across space within the country, region or province. Sub-national analyses not only show which areas are experiencing greater changes in heat exposures, but also shed light on whether aggregate national and regional changes are due to population shifts across regions and across provinces within-region, respectively.[D.1]

In Panel A of Tables D.6 and D.7, we conduct our analysis based on changes in the distribution of children and temperature within each of the four economic regions of China. In successive panels, we present province-specific results based on within-province changes. Table D.6 presents results for at least strong ($\geqslant 32\,^{\circ}$C and $\geqslant 35\,^{\circ}$C) and very strong heat stress ($\geqslant 38\,^{\circ}$C) exposure thresholds across columns. Table D.7 focuses on moderate ($\geqslant 26\,^{\circ}$C and $\geqslant 29\,^{\circ}$C) heat stress thresholds and also provides results for the $\geqslant 23^{\circ}$C threshold.

EDIT PLEASE: *Discuss briefly additional details here, consider changes to main text, ideas*

1. **Eastern increases faster than central**: In 1990, the central region, followed by eastern, had the highest average share of child heat exposure time. Between 1990 and 2020, while central exposure stagnated with 1% to 4% increases (for at least moderate and strong heat stress thresholds), the eastern region experienced increases of 20% to 35% across heat stress thresholds, catching up to the central region. In 2020, the average eastern region child experienced 28.1% and 10.1% of her time under at least moderate ($\geqslant 26\,^{\circ}$C) and at least strong ($\geqslant 32\,^{\circ}$C) heat stress.

2. **Northeastern increase but remains low**: The northeastern region had very low average child heat exposure in 1990, but by 2020, experienced increases of 19% ($\geqslant 26\,^{\circ}$C) and 36% ($\geqslant 29\,^{\circ}$C) for average at least moderate heat stress and 106% ($\geqslant 32\,^{\circ}$C) and 457% ($\geqslant 35\,^{\circ}$C) for at least strong heat stress. In 2020, the average northeastern region child experienced 8.9% and 2.4% of her time under at least moderate ($\geqslant 26\,^{\circ}$C) and at least

D.1. In an extreme scenario, there might be no changes in temperatures and no changes in the distribution of population within regions, but if the overall national population shares in higher heat stress regions increase, average national child heat exposure will increase.

strong ($\geqslant 32\,^{\circ}$C) heat stress, which are still much lower than average exposure levels in Central and Eastern regions.

3. **Top 5 provinces with increasing child heat exposures**: In 2020, Hainan (eastern), Guangdong (eastern), Guangxi (western), Jiangxi (central), and Fujian (eastern) are generally ranked from top 1 to 5 in terms of average share of child time exposed to heat across all UTCI thresholds. Specifically, in 2020, children in Hainan, Guangdong, Guangxi, Jiangxi and Fujian had on average 19.2%, 15.2%, 13.2%, 12.8%, and 11.8% share of time exposed to at least strong heat stress ($\geqslant 32\,^{\circ}$C), which represented 17, 20, 8, 16, and 54 percent increases in share of time exposed compared to 1990.

4. **Some provinces with decreasing or no heat exposures**: While northeastern and eastern provinces (excluding Jiangsu) experienced substantial increases in heat exposures, provinces in central and western regions experienced limited exposure increases and reductions. In particular, central provinces of Hubei and Anhui and western provinces of Shaanxi and Sichuan generally experienced reductions in average child heat exposures across UTCI thresholds. Additionally, children in Qinghai and Xizang (Tibet) in the western region continue to have generally no exposure to at least moderate heat stress.

5. **Provinces with similar percentage points increases**: For at least strong heat stress ($\geqslant 32\,^{\circ}$C), Hebei and Zhejiang in the eastern region, along with all northeastern provinces, all experienced between 1.0 to 1.3 percentage points increases in average share of time heat exposure. Since the northeastern provinces started at much lower levels, the percentage increases in the northeastern provinces are 3 to 15 times larger. Due to heterogeneities across provinces in prior exposure levels, the same percentage points increases represented a much bigger change from the status quo for the northeastern provinces.

6. **Similar 2020 level but different changes** In 2020, the average child experiences having 7.6% and 7.8% of her annual time with at least strong heat stress ($\geqslant 32\,^{\circ}$C) in eastern provinces of Hebei and Jiangsu, respectively. But the Hebei and Jiangsu experienced 17% increase and 11% reductions in heat exposures between 1990 and 2020, respectively. Depending on prior exposure levels, provinces might require different types of societal and physical adjustments despite having the same level of heat exposure today.

D.4.1 Very strong and strong heat stress across regions

Table D.6: Changes in regional average share of time exposed to strong and very strong heat

	At least strong heat stress								Very strong heat stress			
	⩾ UTCI 32° C				⩾ UTCI 35° C				⩾ UTCI 38° C			
	Share of time		Changes		Share of time		Changes		Share of time		Changes	
Location	1990	2020	Level	%	1990	2020	Level	%	1990	2020	Level	%
Panel A: Regions												
Eastern	8.4%	10.1%	1.7pp	20%	3.9%	5.0%	1.1pp	29%	1.0%	1.4%	0.4pp	35%
Northeastern	1.1%	2.4%	1.2pp	106%	0.1%	0.6%	0.5pp	457%	0.0%	0.1%	0.1pp	7.4k%
Central	9.3%	9.6%	0.3pp	3%	4.9%	5.1%	0.2pp	4%	1.7%	1.6%	-0.1pp	-3%
Western	5.7%	5.4%	-0.3pp	-5%	2.6%	2.4%	-0.2pp	-7%	0.8%	0.6%	-0.2pp	-24%
Panel B: Eastern region												
Beijing	2.9%	6.3%	3.4pp	117%	0.5%	2.8%	2.3pp	424%	0.0%	0.6%	0.6pp	1.2k%
Fujian	7.7%	11.8%	4.1pp	54%	2.9%	5.6%	2.7pp	94%	0.5%	1.3%	0.9pp	175%
Guangdong	12.7%	15.2%	2.5pp	20%	5.7%	7.5%	1.8pp	31%	1.3%	2.0%	0.7pp	56%
Hainan	16.3%	19.2%	2.8pp	17%	6.4%	10.0%	3.6pp	57%	0.9%	3.4%	2.4pp	261%
Hebei	6.5%	7.6%	1.1pp	17%	2.9%	3.9%	1.0pp	34%	0.8%	1.0%	0.2pp	31%
Jiangsu	8.7%	7.8%	-0.9pp	-11%	4.7%	3.8%	-0.9pp	-20%	1.7%	1.3%	-0.4pp	-25%
Shandong	6.8%	7.1%	0.4pp	6%	2.9%	3.3%	0.4pp	13%	0.5%	0.9%	0.3pp	58%
Shanghai	6.8%	6.1%	-0.7pp	-10%	3.1%	2.7%	-0.4pp	-14%	1.0%	0.6%	-0.4pp	-40%
Tianjin	5.6%	7.3%	1.7pp	31%	2.1%	3.8%	1.7pp	84%	0.2%	0.9%	0.7pp	308%
Zhejiang	8.2%	9.2%	1.0pp	12%	4.6%	4.9%	0.4pp	8%	1.9%	1.6%	-0.3pp	-14%
Panel C: Northeastern region												
Heilongjiang	0.6%	1.7%	1.1pp	175%	0.0%	0.4%	0.4pp	1.6k%	0.0%	0.0%	0.0pp	
Jilin	0.8%	2.1%	1.3pp	148%	0.0%	0.5%	0.5pp	2.7k%	0.0%	0.0%	0.0pp	
Liaoning	1.9%	2.9%	1.1pp	56%	0.3%	0.8%	0.6pp	216%	0.0%	0.1%	0.1pp	4.5k%
Panel D: Central region												
Anhui	10.1%	9.3%	-0.8pp	-7%	5.8%	5.0%	-0.9pp	-15%	2.2%	1.8%	-0.4pp	-18%
Henan	8.9%	9.5%	0.6pp	7%	4.5%	5.1%	0.5pp	12%	1.4%	1.6%	0.2pp	13%
Hubei	10.2%	9.3%	-0.9pp	-9%	5.5%	4.9%	-0.6pp	-10%	2.0%	1.3%	-0.7pp	-35%
Hunan	10.2%	10.6%	0.4pp	4%	5.0%	5.4%	0.4pp	7%	1.6%	1.6%	0.0pp	0%
Jiangxi	11.0%	12.8%	1.8pp	16%	6.1%	7.4%	1.2pp	20%	2.4%	2.9%	0.5pp	19%
Shanxi	2.6%	2.8%	0.1pp	5%	0.8%	0.7%	-0.1pp	-18%	0.2%	0.1%	-0.1pp	-53%
Panel E: Western region												
Gansu	0.8%	0.8%	0.0pp	-1%	0.1%	0.1%	0.0pp	-17%	0.0%	0.0%	0.0pp	-17%
Guangxi	12.3%	13.2%	1.0pp	8%	5.5%	6.6%	1.1pp	20%	1.5%	1.4%	-0.1pp	-7%
Guizhou	2.8%	2.1%	-0.7pp	-26%	0.7%	0.3%	-0.4pp	-53%	0.1%	0.0%	0.0pp	-54%
Neimenggu	0.9%	2.0%	1.1pp	116%	0.1%	0.6%	0.4pp	296%	0.0%	0.1%	0.1pp	268%
Ningxia	2.1%	2.8%	0.7pp	31%	0.7%	0.9%	0.2pp	35%	0.1%	0.1%	0.0pp	17%

Continued on next page

Table D.6: Changes in regional average share of time exposed to strong and very strong heat

	At least strong heat stress								Very strong heat stress			
	⩾ UTCI 32° C				⩾ UTCI 35° C				⩾ UTCI 38° C			
	Share of time		Changes		Share of time		Changes		Share of time		Changes	
Location	1990	2020	Level	%	1990	2020	Level	%	1990	2020	Level	%
Qinghai	0.0%	0.0%	0.0pp		0.0%	0.0%	0.0pp		0.0%	0.0%	0.0pp	
Shaanxi	4.6%	4.3%	-0.4pp	-8%	1.9%	1.5%	-0.4pp	-23%	0.6%	0.2%	-0.3pp	-58%
Sichuan	8.0%	7.4%	-0.7pp	-8%	4.2%	3.6%	-0.6pp	-14%	1.3%	1.0%	-0.3pp	-23%
Xinjiang	4.3%	5.2%	0.9pp	22%	2.0%	2.4%	0.4pp	19%	0.7%	0.7%	0.0pp	0%
Xizang	0.0%	0.0%	0.0pp		0.0%	0.0%	0.0pp		0.0%	0.0%	0.0pp	
Yunnan	0.9%	1.2%	0.3pp	33%	0.1%	0.1%	0.0pp	53%	0.0%	0.0%	0.0pp	-7%

Note: We present similar statistics as in Table D.1, but now compute exposures separately for four economic regions and provincial-level administrative units in China. Columns (cols) 1–3 and 4–6 focus on at least strong UTCI heat exposure at ⩾ 32 °C and ⩾ 35 °C, respectively. Cols 7–9 focus on very strong UTCI heat exposure at ⩾ 38 °C. Cols 1 and 2, 5 and 6, and 9 and 10 show the annual average shares of time that children in China (ages 0–14) are exposed to UTCI temperatures at ⩾ z °C. Cols 3 and 4, 7 and 8, and 11 and 12 show 1990 to 2020 changes in percentage points (level) or percentage (%) of the average shares of time exposed to heat. Cells are empty for percentage changes when the denominator is equal to zero. We consider all 24 hours and 12 months.

D.4.2 Moderate and no heat stress across regions

Table D.7: Changes in regional average share of time exposed to moderate heat

	At least borderline thermal stress				At least moderate heat stress							
	⩾ UTCI 23° C				⩾ UTCI 26° C				⩾ UTCI 29° C			
	Share of time		Changes		Share of time		Changes		Share of time		Changes	
Location	1990	2020	Level	%	1990	2020	Level	%	1990	2020	Level	%
Panel A: Regions												
Eastern	33.8%	37.0%	3.2pp	9%	23.6%	28.1%	4.4pp	19%	14.3%	17.1%	2.8pp	20%
Northeastern	12.0%	13.5%	1.5pp	13%	7.5%	8.9%	1.4pp	19%	3.8%	5.2%	1.4pp	36%
Central	32.0%	32.7%	0.7pp	2%	23.4%	23.6%	0.2pp	1%	15.1%	15.5%	0.4pp	3%
Western	25.6%	25.3%	-0.3pp	-1%	17.1%	17.2%	0.2pp	1%	10.2%	10.0%	-0.2pp	-2%
Panel B: Eastern region												
Beijing	19.0%	23.2%	4.3pp	23%	12.1%	16.2%	4.1pp	34%	7.0%	10.7%	3.7pp	53%
Fujian	38.9%	45.6%	6.7pp	17%	24.6%	32.5%	7.9pp	32%	14.1%	19.0%	4.9pp	35%
Guangdong	51.9%	55.5%	3.7pp	7%	37.5%	45.3%	7.8pp	21%	21.6%	26.3%	4.7pp	22%
Hainan	63.5%	63.4%	0.0pp	0%	47.1%	51.8%	4.7pp	10%	27.7%	31.5%	3.9pp	14%
Hebei	24.4%	25.1%	0.7pp	3%	17.0%	18.0%	1.0pp	6%	10.8%	12.3%	1.5pp	14%
Jiangsu	30.5%	29.7%	-0.8pp	-3%	22.5%	21.5%	-1.0pp	-4%	14.3%	13.7%	-0.6pp	-4%
Shandong	26.7%	25.3%	-1.4pp	-5%	18.1%	18.2%	0.0pp	0%	11.4%	12.1%	0.7pp	6%
Shanghai	27.9%	29.7%	1.8pp	7%	19.7%	20.7%	1.0pp	5%	12.3%	11.3%	-1.0pp	-8%
Tianjin	23.5%	25.2%	1.7pp	7%	15.8%	17.8%	1.9pp	12%	9.7%	12.1%	2.3pp	24%

Continued on next page

Table D.7: Changes in regional average share of time exposed to moderate heat

	At least borderline thermal stress				At least moderate heat stress							
	⩾ UTCI 23° C				⩾ UTCI 26° C				⩾ UTCI 29° C			
	Share of time		Changes		Share of time		Changes		Share of time		Changes	
Location	1990	2020	Level	%	1990	2020	Level	%	1990	2020	Level	%
Zhejiang	33.4%	36.0%	2.6pp	8%	22.6%	26.5%	3.9pp	17%	13.6%	15.4%	1.8pp	13%
Panel C: Northeastern region												
Heilongjiang	10.2%	11.2%	1.0pp	9%	6.3%	7.3%	0.9pp	15%	2.9%	4.0%	1.1pp	38%
Jilin	11.1%	12.2%	1.1pp	10%	6.9%	8.5%	1.5pp	22%	3.4%	4.9%	1.5pp	45%
Liaoning	14.4%	15.8%	1.4pp	10%	9.1%	10.3%	1.3pp	14%	5.1%	6.2%	1.1pp	21%
Panel D: Central region												
Anhui	32.7%	32.3%	-0.4pp	-1%	25.2%	23.4%	-1.8pp	-7%	16.2%	15.5%	-0.7pp	-5%
Henan	29.6%	29.4%	-0.2pp	-1%	21.5%	21.1%	-0.4pp	-2%	13.9%	14.5%	0.6pp	4%
Hubei	33.3%	33.9%	0.6pp	2%	25.1%	24.2%	-0.9pp	-3%	16.7%	15.4%	-1.3pp	-8%
Hunan	36.2%	37.6%	1.4pp	4%	25.7%	26.8%	1.1pp	4%	16.5%	17.1%	0.5pp	3%
Jiangxi	38.8%	41.8%	3.0pp	8%	28.1%	31.7%	3.6pp	13%	17.9%	20.9%	3.1pp	17%
Shanxi	16.1%	16.6%	0.5pp	3%	10.6%	11.1%	0.6pp	5%	6.0%	6.6%	0.5pp	9%
Panel E: Western region												
Gansu	11.1%	10.7%	-0.4pp	-3%	6.6%	6.4%	-0.2pp	-3%	3.0%	2.9%	0.0pp	-1%
Guangxi	47.5%	49.2%	1.7pp	4%	33.3%	36.8%	3.4pp	10%	20.2%	21.4%	1.2pp	6%
Guizhou	19.5%	19.4%	-0.1pp	0%	12.2%	11.6%	-0.6pp	-5%	7.0%	6.1%	-0.9pp	-13%
Neimenggu	9.9%	12.0%	2.1pp	21%	6.0%	8.2%	2.2pp	36%	2.9%	4.7%	1.8pp	62%
Ningxia	12.9%	14.1%	1.1pp	9%	8.8%	9.6%	0.8pp	10%	5.0%	5.7%	0.7pp	13%
Qinghai	4.9%	3.8%	-1.1pp	-23%	1.4%	1.0%	-0.4pp	-30%	0.1%	0.0%	-0.1pp	-71%
Shaanxi	19.5%	19.3%	-0.2pp	-1%	13.3%	13.1%	-0.3pp	-2%	8.6%	8.2%	-0.3pp	-4%
Sichuan	28.5%	29.4%	0.8pp	3%	19.3%	19.7%	0.4pp	2%	12.5%	12.2%	-0.3pp	-3%
Xinjiang	16.3%	18.0%	1.6pp	10%	11.4%	13.1%	1.7pp	14%	7.4%	8.8%	1.4pp	18%
Xizang	1.3%	1.4%	0.1pp	5%	0.1%	0.1%	0.0pp	-32%	0.0%	0.0%	0.0pp	159%
Yunnan	19.2%	21.0%	1.8pp	9%	11.0%	12.3%	1.3pp	12%	4.6%	5.3%	0.8pp	17%

Note: We present similar statistics as in Table D.1, but now compute exposures separately for four economic regions and provincial-level administrative units in China. Columns (cols) 4–6 and 7–9 focus on at least moderate UTCI heat exposure at $\geqslant$ 26 °C and $\geqslant$ 29 °C, respectively. Cols 1–3 provide UTCI heat exposure at $\geqslant$ 23 °C, where UTCI 23 °C is a temperature level that is just below the threshold (25 °C) for moderate heat stress. Cols 1 and 2, 5 and 6, and 9 and 10 show the annual average shares of time that children in China (ages 0–14) are exposed to UTCI temperatures at $\geqslant z$ °C. Cols 3 and 4, 7 and 8, and 11 and 12 show 1990 to 2020 changes in percentage points (level) or percentage (%) of the average shares of time exposed to heat. Cells are empty for percentage changes when the denominator is equal to zero. We consider all 24 hours and 12 months.